SOUTHEASTERN GEOLOGY

PUBLISHED AT DUKE UNIVERSITY DURHAM, NORTH CAROLINA

VOL. 24, NO. 1 MAY, 1983

SOUTHEASTERN GEOLOGY

PUBLISHED QUARTERLY

AT

DUKE UNIVERSITY

This journal welcomes original papers on all phases of geology, geophysics, and geochemistry as related to the Southeast. Transmit manuscripts to S. DUNCAN HERON, JR., BOX 6665, COLLEGE STATION, DURHAM, NORTH CAROLINA 27708. Observe the following:

1) Type the manuscript with double space lines and submit in duplicate.
2) Cite references and prepare bibliographic lists in accordance with the method found within the pages of this journal.
3) Submit line drawings and complex tables as finished copy.
4) Make certain that all photographs are sharp, clear, and of good contrast.
5) Stratigraphic terminology should abide by the code of Stratigraphic Nomenclature (AAPG, v. 45, 1961).

Proofs will be sent authors.

Reprints must be ordered prior to publication; prices available upon request. Subscriptions to Southeastern Geology are $8.00 per volume (US and Canada) $10.00 per volume (foreign). Inquiries should be sent to: SOUTHEASTERN GEOLOGY, BOX 6665, COLLEGE STATION, DURHAM, NORTH CAROLINA 27708. Make checks payable to: Southeastern Geology.

SOUTHEASTERN GEOLOGY

Table of Contents

Vol. 24, No. 1

May, 1983

PETROLOGY AND DIAGENESIS OF THE RAVENCLIFF SANDSTONE IN WEST VIRGINIA

By

M. W. Kamm
Chevron USA
111 Tulane Avenue
New Orleans, Louisiana 70112

And

M. T. Heald
Department of Geology and Geography
West Virginia University
Morgantown, West Virginia 26506

ABSTRACT

The Ravencliff sandstone of upper Mississippian age is an important gas producer and occurs in the subsurface in a long linear trend in southern West Virginia. The sandstone is a quartz arenite and ranges in thickness from 50 to 100 feet in the study area. The sandstone is apparently of fluvial origin with common cross-bedding and pebbly zones. The base of the sandstone is in sharp contact with underlying limestone or shale but the upper contact is more gradational.

The original high porosity of the sandstone was reduced by a variety of diagenetic processes with quartz cementation and pressure solution being the most important. Some of the lowest porosity occurs where illite promoted intense pressure solution. Calcite cement is minor except near the base of the sandstone where it commonly fills pores completely. Kaolinite which occurs in some pores tended to block quartz growth and has small voids between its characteristic books.

Leaching increased porosity to a small extent particularly by partial dissolution of feldspar and calcite. In some specimens, phyllosilicate inclusions within detrital grains were leached. Some of the quartz grains also appear to have undergone partial dissolution.

The highest porosity in the Ravencliff sandstone is generally in the coarser intervals where initial clay content was low and the larger pores were less affected by quartz cementation and pressure solution. Furthermore, greater circulation in the coarser sandstone apparently promoted leaching of unstable components.

INTRODUCTION

The Ravencliff interval is composed mainly of a series of sandstones, gray shales and siltstones occurring in the subsurface along a trend from Nicholas to McDowell County, West Virginia. The basal sand of the series has proven to be an attractive natural gas reservoir and is normally thicker and more continuous than the overlying sandstones. The petrology and diagenesis of this gas producing sand is the subject of this investigation and will be referred to as the Ravencliff sandstone.

Stratigraphically, the Ravencliff member (informal) comprises the upper part of the Hinton Formation (Mauch Chunk Group, Upper Mississippian Series) and consists of strata between the top of Avis Limestone, or Little Stone Gap member and the bottom of the Bluestone Formation (Schalla, 1980).

Most of the data for this study were obtained from two cores provided by Appalachian Exploration and Development, Inc. The cores were from the David Bell well #1 (Nic. 445) in Nicholas County and the Wriston well #1 (Ral. 460) located in Raleigh County. Core examination was supplemented by 35 thin sections cut from selected intervals of the cores. Mineral percentages were determined from approximately 300 point counts per slide. The mean grain size and sorting were obtained by measuring 75 to 100 grains in each slide. Cuttings and electric logs from two

additional wells in Nicholas County and one well in Raleigh County were included in the study. Radiographs of slabs of the Wriston core were prepared to study subtle textures and sedimentary structures in the sandstone. Figure 1 shows the location of the wells studied and approximate extent of the Ravencliff sandstone in West Virginia as proposed by Donaldson and Shumaker (1979).

GENERAL LITHOLOGY

The Ravencliff sandstone ranges from 50 to 100 feet thick in the study area. Cores taken from the sandstone at the Wriston and David Bell wells are 56 and 66 feet thick respectively. Although nearly 30 miles apart, the sandstone observed in these two cores is remarkably similar. Generally composed of a clean, white to tan colored quartz sandstone, the unit is best classified as a quartz arenite or orthoquartzite. Some feldspar, argillaceous material, heavy minerals, and rock fragments were also initially deposited in the sand as well as trace amounts of organic material mostly in the form of plant fragments.

Framework grains range from fine to coarse with the majority generally being medium in size. Most were initially well rounded and typically show a high degree of sphericity. Secondary growth and pressure solution have since altered the grains; however, thin dust rims on some grains reveal the original grain shape. Quartz pebbles up to two centimeters in diameter are present throughout much of the sand and are locally concentrated along distinct zones, forming conglomerates. Clay clasts are also incorporated in the sandstone and commonly occur within the pebbly zones. A few of the larger clasts are angular and suggest a short distance of transport before redeposition.

The longest intercepts of grains as seen in thin section were measured for grain size determinations. Sorting values were determined for the two cores using Folk's inclusive graphic standard deviation procedure (Table 1). Average values of .54ϕ and .66ϕ were established from the David Bell and Wriston cores respectively with about

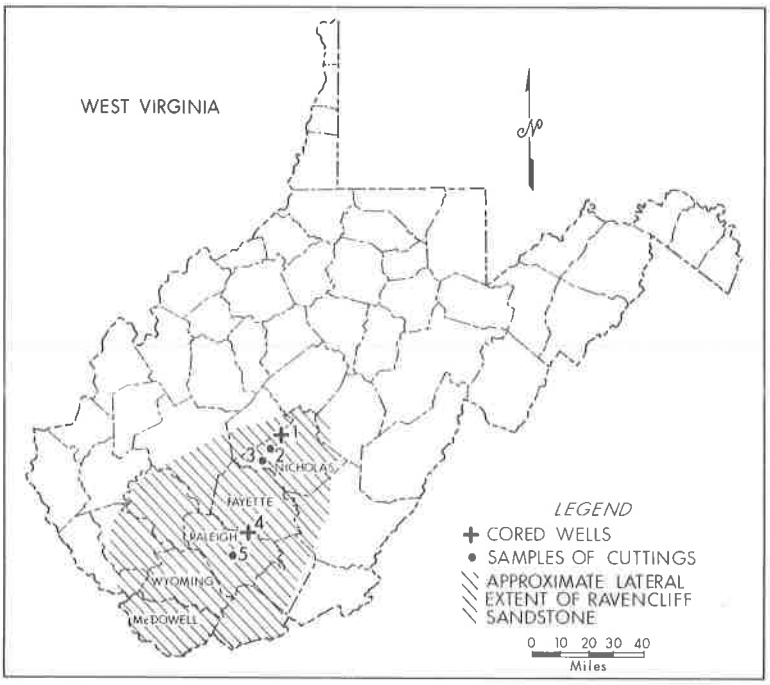

Figure 1. Location of wells studied and approximate lateral extent of the Ravencliff sandstone. 1) David Bell (Nic. 445), 2) Ridgeway #1 (Nic. 481), 3) Richardson #1 (Nic. 490), 4) Wriston #1 (Ral. 460), 5) Beaver Coal #A-19 (Ral. 483).

Table 1. Composition, porosity, and texture of Ravencliff Sandstone, Bell well #1 (Nic-445) Nicholas County, West Virginia.

	1	2	3	4	5	6	7
Quartz %	90.0	77.2	88.7	90.2	91.0	71.6	87.5
Feldspar %	1.5	0.9	1.0	0.5	0.9	tr	0.3
Carbonate %	1.0	tr	0.9	0.3	3.0	26.2	tr
Kaolinite %	1.1	1.7	1.9	1.0	0.4	tr	5.5
Illite %*	5.8	19.9	2.5	1.2	0.4	1.7	6.4
Miscellaneous %	0.2	0.3	tr	tr	tr	0.5	3
Porosity %**	0.4	0	5.0	6.8	4.3	tr	
Mean Grain Size (mm)	0.21	0.20	0.26	0.46	0.46	0.47	0.42
Sorting Coefficient, σ_I	0.54	0.54	0.41	0.52	0.44	0.83	0.45

*Includes miscellaneous phyllosilicates
**Porosity as observed in thin section

Samples grouped according to similarity in porosity/permeability and lithology

1) Low porosity, low permeability intervals. Average of samples at 1141' and 1144'. 2) Low porosity from closely spaced argillaceous laminations and stylolite seams at 1157'. 3) Moderate porosity and moderate permeability intervals. Average of samples at 1154', 1161' and 1179'. 4) Moderate porosity and relatively high permeability intervals. Average of samples at 1138', 1164', 1170' and 1175'. 5) Carbonate in patches. Moderate porosity and high permeability at 1193'. 6) Intervals tightly cemented with carbonate. Average of samples at 1199' and 1203'. 7) Intervals with abundant shale clasts. Low porosity and low permeability. 1189'.

Core depths adjusted to correspond to depths on gamma ray log.

half of the samples being moderately well sorted and most of the remainder being well sorted. Extreme values range from very well sorted to poorly sorted. No definite correlation was apparent between grain size and sorting.

Sedimentary structures observed from radiographic images of the Wriston core indicate that 63 percent of the sand is characterized by cross-beds inclined from one to thirty degrees, with the remaining 37 percent being horizontally bedded or showing no distinct sedimentary features. Thin bands of heavy minerals and/or argillaceous material, as well as interbedding of fine, medium, and coarse sand accentuate the bedding in most cases. Identifying the type of cross-bedding is difficult from only core samples but accretion and some avalanche cross-bed sets appear to be present. In many instances, horizontal bedding seems to truncate cross-beds below. The cross-bedding appears to be predominantly unidirectional as few reversals are seen in unbroken segments of the core; however, the direction of these flow features is unknown because the cores were not oriented. Very coarse pebbly zones, which are more common in the lower part of the sandstone, normally show no bedding or in some places a vague horizontal bedding.

In most wells, grain size of the sandstone becomes finer from bottom to top. Pawlowski (1975) and Oliva (1976) also recognized the fining upward grain size of the Ravencliff sandstone. Because clay is generally high in natural radiation and commonly increases in amount with decreasing grain size, this fining upward trend is also suggested by the characteristic "Christmas tree" signature of most gamma ray logs of the Ravencliff sandstone. A positive correlation between decreasing grain size and increasing clay content was recognized in many samples; however, clay clasts occur in many of the coarser pebbly intervals because of rip up of clay layers by stronger currents. The overall fining upward trend and associated increase in detrital clays as plotted from thin section data of the David Bell core are shown in Figure 2.

DEPOSITIONAL ENVIRONMENT

Until recently, the depositional setting of the Ravencliff sandstone was poorly understood. The linear nature of this clean sandstone could be explained either as a marine unit or a fluvial one. Support for a marine barrier-bar or beach origin probably

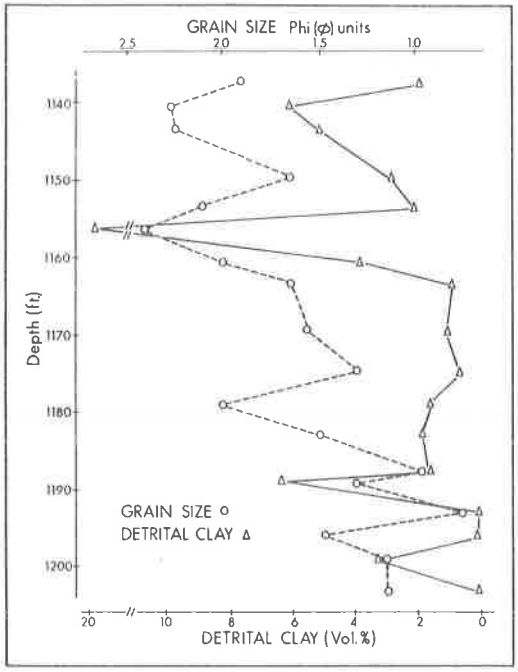

Figure 2. Variation in grain size and detrital clay based on thin sections from the David Bell core.

was formulated as a result of the close association with the underlying Avis Limestone, a known marine unit and high quartz content of the sand.

Additional data have led to the now generally preferred fluvial-fluvial deltaic depositional model for the Ravencliff. Schalla (1980) feels that the southern extension of the Ravencliff interval in McDowell County represents the delta complex of a southward trending fluvial system in which there were three essentially contemporaneous environments of deposition: 1) delta-plain and distributary; 2) delta front and shoreline; 3) delta platform and prodelta.

Wrightstone (personal communication) also studied the Ravencliff in McDowell County and adjacent Wyoming County and believed that the interval represents a regressive phase of deposition, from the marine Avis Limestone environment to a shoreline/beach environment and then to a deltaic-fluvial environment with anastomosing subbelts of individual fluvial sandstones making up most of the interval. Although both Wrightstone and Schalla studied the Ravencliff sandstone primarily in McDowell County, their reconnaissance work in Raleigh and Nicholas Counties led them to conclude that the Ravencliff in these counties was fluvial. Donaldson and Shumaker (1979) believed that the Ravencliff sandstone formed from a braided to meandering river system which supplied sediment to its delta downstream near the state boundary in southern West Virginia.

The sudden shifting of depositional centers typically associated with deltaic sedimentation possibly accounts for the occurrence of more multistacked sands in McDowell County. The Ravencliff sandstone in the study area is more uniform and massive, but generally is not as thick as in McDowell County as might be expected in a predominantly fluvial environment. Here reworking and winnowing out of finer sediments by laterally shifting streams would characterize a more slowly subsiding area. The basal contact of the sandstone is extremely sharp and has been interpreted to be erosional as the thickness of the sandstone varies inversely with thickness of the Avis Limestone in McDowell and Wyoming Counties (Wrightstone, personal communication).

The roundness of detrital grains, occasional pebbly zones, moderately good sorting, and lack of significant amounts of detrital argillaceous material (normally less

than 5 percent) indicate a rather high energy depositional environment which could be either fluvial or marine. However, the occurrence of angular gray clay clasts, with some as much as 8 centimeters across, within some of the pebbly zones in the cores strongly supports the idea of fluvial deposition inasmuch as clay clasts, in general, are more characteristic of fluvial sedimentation (Donaldson, personal communication). The clay clasts could not possibly have been transported a substantial distance and have been interpreted to represent small amounts of dislodged overbank material.

Steeply dipping cross-beds, such as those occurring within the Ravencliff, are typically more indicative of fluvial than marine deposition. Marine barrier-bar and beach sands typically show low angle or horizontal bedding with cross-bedding being more multi-directional (Donaldson, personal communication; Pryor, 1960).

Thus the sedimentary structures, large clay clasts, sharp erosional basal contact and fining upward trend support the idea of a fluvial origin for the Ravencliff sandstone. The lack of marine indicators such as glauconite and marine fossils is in harmony with this interpretation.

CLASTIC CONSTITUENTS

Quartz grains are typically clean but some contain numerous tiny inclusions creating a dusty cast similar to slightly altered feldspar. Larger inclusious of vermicular chlorite and other phyllosilicates are also present in some grains especially in the polycrystalline quartz. Most of the monocrystalline quartz shows uniform to slightly undulose extinction although some is highly undulose. About 5 percent of the quartz grains are polycrystalline and have elongate constituent crystals which are without much question of metamorphic origin. The detrital grains were initially fairly spherical and well rounded but have since been modified by pressure solution, replacement and secondary growth. The detrital cores of some grains are clearly outlined by dust rings, but this is not common.

Feldspar generally constitutes less than 1 percent of the sandstone and is represented by orthoclase and plagioclase. Most of the feldspar shows slight alteration with small sericite flakes forming particularly along cleavage planes. Plagioclase exhibits more alteration than orthoclase and occurs in somewhat smaller and more angular grains than the other constituents. This apparently is a result of more breakage on transport perhaps because of weakness from incipient alteration along cleavage planes.

Lithic grains are represented by chert, shale, slate, micaceous quartzite and fine-grained schist but constitute only a small percentage of the sandstone. Detrital illite is the chief constituent in the argillaceous laminations and additionally occupies some interstices especially near the laminations. Individual flakes of muscovite and biotite occur in trace amounts. Clay clasts which have been compacted into lenticular forms are commonly fractured, with kaolinite present between the resulting fragments. The kaolinite formed late as spaces occur between books and there is no evidence of compaction.

DIAGENESIS

Cementation

Quartz is the chief cement in most of the Ravencliff sandstone. The exact amount of secondary quartz could not be ascertained under the petrographic microscope because dust rings were not consistently developed. However, euhedral faces along pores and straight contacts between grains in many cases indicated that quartz growth was widespread. Sizeable growths were apparent in those samples with dust rings.

Secondary overgrowths on feldspar are small and characteristically are free of inclusions and twinning.

Carbonate cement ranged from 26 percent in the basal 6 or 7 feet of the sandstone to a trace in some of the upper sections with an average content of about 1 percent. Both calcite and dolomite are present but calcite is much more common. In slides with appreciable carbonate, Alizarin red stain indicated that calcite constituted about 96 percent of the total carbonate; however, in some areas, dolomite

result in concave-convex and sutured contacts. Although only a small amount of material dissolves at a given contact, the total amount may be appreciable especially in the finer beds where there are many more contacts in a given layer. Some of this dissolved material may furnish an important part of the cement in the Ravencliff sandstone.

Dissolution

Conditions were conducive for dissolution of some minerals in the Ravencliff sandstone. Partial dissolution of calcite is indicated in the middle intervals especially in the Bell well. Former presence of calcite is presumed in pores where at least some of the quartz grains have ragged margins (Pl. 1C) similar to those resulting from corrosion by calcite. Not all irregular margins are from calcite attack, but deep embayments particularly with reentrants are suggestive of replacement by calcite that was subsequently leached. The middle interval was never tight as many pores show no evidence of removal of calcite so circulation was apparently favorable for leaching of calcite. Where calcite tightly cemented the sandstone as at the base of the Bell well, leaching did not occur presumably because of low permeability.

Although dissolution of phyllosilicates in the subsurface has not been previously reported, it appears to have occurred in the Ravencliff sandstone in spite of the fact that phyllosilicates are generally considered to be relatively stable. The voids within some of the quartz grains are best explained as a result of dissolution of inclusions of phyllosilicates. Because of the greater solubility of carbonate, it might seem likely that carbonate inclusions had been leached. However, most of these voids are smaller than the typical calcite inclusions in quartz. Furthermore, some of the quartz grains with the most extensive voids are surrounded by carbonate which shows no evidence of leaching. Where dissolution has not occurred, there are grains of fine-grained micaceous quartzite and monocrystalline quartz with inclusions of phyllosilicates of the same size and distribution as the voids within quartz. Removal of these phyllosilicates would produce the observed voids within the grains. In some quartz grains the dissolution is incomplete with voids in the outer margin of the quartz and phyllosilicate inclusions in the interior of the grains. The unique shape of the voids resulting from removal of vermicular phyllosilicates is clear evidence that phyllosilicates were undergoing dissolution (Pl. 1B). Further support for the idea of dissolution of phyllosilicates is indicated by the occurrence of tiny pyrite grains within some of the voids. Inasmuch as pyrite preferentially replaces phyllosilicates in the Ravencliff sandstone, it appears that the pyrite is a residue left after the dissolution of the phyllosilicates. The removal of the phyllosilicates could not have been predepositional because some grains are laced with voids and would have been too fragile for transport. The phyllosilicates that dissolved in the subsurface apparently were varieties of mica and chlorite which were less stable than the interstital illite which was not affected.

About half of the feldspar grains showed clear evidence of dissolution. All degrees of dissolution of feldspar could be observed from slight corrosion to nearly complete removal of grains. Some of the voids with the shape of detrital feldspar are undoubtedly molds resulting from complete dissolution. Both potash feldspar and plagioclase were attacked but secondary feldspar overgrowths resisted dissolution (Pl. 1D).

There is some indication that quartz has also undergone dissolution. Most of the quartz is unaffected but some of the highly strained quartzite grains and quartz with many fluid inclusions apparently were partially leached. The voids are smaller and have a more intricate pattern (Pl. 1E) than inclusions of either calcite or phyllosilicates so that it is unlikely that removal of these constituents produced the voids. Circulation was required for the dissolution as it was most extensive in porous zones particularly in the Wriston well.

SEQUENCE OF DIAGENETIC EVENTS

Mechanical compaction was the first diagenetic process and resulted in tighter packing of detrital components with accompanying deformation of mechanically weak ductile grains such as those rich in phyllosilicates. The fact that these grains were

squeezed into pores free of authigenic minerals indicates that the compaction preceded secondary growth. Mechanical adjustments to overburden load eventually slowed and chemical compaction in the form of pressure solution occurred along stylolite seams and between individual grain contacts.

Small amounts of secondary quartz and feldspar, nucleating on unobstructed surfaces of detrital grains, appear to have been the first authigenic minerals to form in most of the Ravencliff. Early authigenic formation of quartz and feldspar apparently occurred concurrently with pressure solution because overgrowths are partly pressolved in some areas. Quartz growth appears to have continued after pressure solution between grains had diminished because much of the secondary quartz is free of pressure solution effects (except along stylolite seams). Support from overgrowths probably is responsible for decreased pressure solution at grain contacts. Completely developed overgrowths are commonly pressolved along stylolite seams indicating that solution along the seams remained effective beyond the period of secondary quartz and feldspar development.

Immediately following the onset of quartz overgrowth was the formation of authigenic kaolinite within interstitial pores. Typically this resulted in kaolinite being in contact with detrital quartz or very near the detrital surface with only small amounts of intervening freely developed authigenic quartz present. The majority of secondary quartz formed after kaolinization. This is suggested by the irregular contact between most quartz and kaolinite as a result of the continued growth of quartz into small voids between individual kaolinite books and substantiated by the fact that significantly larger overgrowths normally occur on grains where neighboring interstices are free of kaolinite.

Authigenic calcite formed in at least two stages. The early calcite began to crystallize at about the same time as secondary quartz but its formation was complete before the bulk of the secondary quartz crystallized. Most of the early diagenetic calcite formed soon after kaolinite, and like kaolinite, is either in contact with detrital quartz grains or with very little intervening secondary quartz. The early calcite most commonly occurs within the basal 6 to 7 feet of the unit where it fills nearly all interstices between detrital grains. In the upper sections of the sandstone, early calcite is rare and occurs only in isolated patches. Evidence supporting the time relationship between early calcite and kaolinite is not always clear. Although all interstices are nearly completely filled by early calcite near the base of the sandstone, close examination reveals that kaolinite had preceded calcite. The kaolinite was nearly completely replaced by calcite leaving ghost structures and some very small inclusions of kaolinite within the calcite. In other areas near the base of the sand where early calcite cementation is less complete and/or kaolinite excessively common, some distinct patches of kaolinite remain and partial replacement by early calcite is more obvious. A 6 mm thick section in which nearly all interstices are filled with kaolinite occurs at the very base of the sandstone overlying a stylolite seam in the Wriston core. The occurrence of this zone in an area characterized by early calcite further suggests that early kaolinite completely filled pores and prevented the formation of calcite.

During later diagenesis, after quartz formation was complete, a second period of calcite formation occurred. The late calcite crystallized in isolated patches which are widely distributed throughout the sandstone but are less common in the basal section where most interstices were previously filled by earlier calcite and secondary quartz. The late calcite is identical in appearance to that formed earlier, but typically occurs in smaller patches as a result of pore size reduction resulting from earlier quartz overgrowth.

Dolomite is apparently the last authigenic mineral to have formed within the sandstone. Minor dolomitization of calcite occurred in some areas as well as precipitation of small patches of dolomite in pores. The last diagenetic event appears to have been dissolution which involved feldspar, phyllosilicates, calcite and quartz. Evidence that dissolution was late is indicated by the fact that authigenic minerals rarely occupy the pore space formed by dissolution. In addition, no extensive fracturing or collapse occurred even in grains highly laced with voids suggesting that dissolution probably occurred after most of the compaction had occurred.

The proposed sequence of diagenetic events is shown graphically in Figure 3.

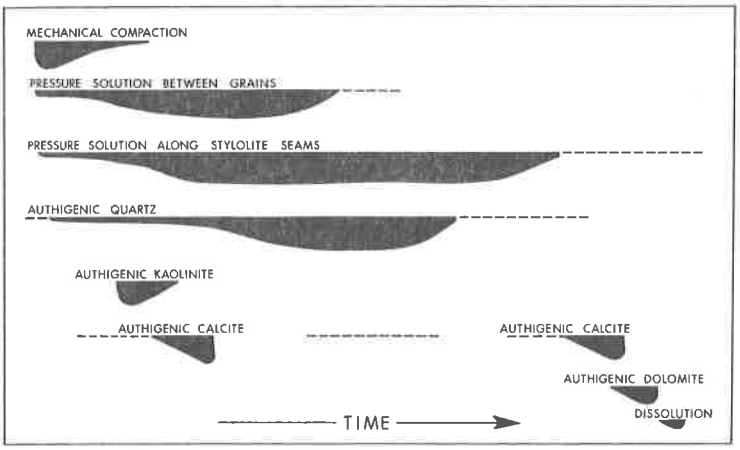

Figure 3. Sequence of diagenetic events.

EFFECTS OF DIAGENESIS ON POROSITY

Initially, the porosity of the Ravencliff sandstone was high as a result of being composed primarily of moderately well-sorted quartz grains and only small amounts of argillaceous material. The two basal samples from the Bell core indicated that initial porosity was high. In these samples early authigenic calcite filled interstitial pores before the sand was highly compacted or cemented with quartz and feldspar. The porosity plus cement in these samples averaged 26 percent. Initially most of the Ravencliff sand would have had a porosity higher than 26 percent because it is generally better sorted than the basal calcite-bearing sand.

Porosity-related diagenesis may be considered under factors tending to (1) decrease porosity (2) preserve porosity and (3) increase porosity. Porosity comparisons are based on voids observed in thin section unless otherwise indicated. These values are about 4 percent lower than those determined by core analysis because the latter include submicroscopic pores.

Most of the diagenetic changes tended to reduce original porosity in the sandstone with the most influential changes being cementation by secondary quartz and pressure solution. Quartz overgrowth is the main porosity reducing cement within the unit except in the basal few feet where calcite is the only cement. Quartz cementation is slightly more effective in decreasing porosity in the finer clean sands because surface area for nucleation is greater and the smaller pores are more readily filled by relatively small growths. However, a few areas of coarse quartz appear to have slightly more secondary quartz than the finer sands. Polycrystalline quartz has small or insignificant overgrowths because of the small size and diverse orientation of the constituent grains which acted as nuclei. For this reason some of the larger pores border polycrystalline quartz. No relationship between silica cementation and depth was recognized. Few overgrowths occur on feldspar grains and do not affect porosity to any significant extent.

Carbonate cement is a major factor in reducing porosity near the base of the sand but is only a minor influence in the rest of the unit where it occurs in isolated patches. Both thin section measurement and core analysis indicate a porosity of less than 0.5 percent in the calcite cemented lower 7 feet of the Bell well.

Mechanical compaction resulted in some porosity loss where detrital grains of ductile phyllosilicates were deformed and squeezed into adjacent pores creating a pseudomatrix. Scattered ductile grains surrounded by supporting quartz grains had little detrimental effect. The same number of ductile grains concentrated more along layers, without supportive quartz grains, underwent compaction with attending porosity loss.

In the few zones where clays are concentrated along thin partings with intervening clean sand, stylolite seams formed and reservoir thickness decreased but interstitial porosity in the sand was generally little affected by the stylolitic solution.

The clay along the stylolite seams mainly accounts for the vertical permeability of less than 0.5 millidarcies in these zones. Most of the beds with clay partings also tend to have additional clay fairly evenly dispersed through the sand. With dispersed clay, porosity is reduced not only by the clay in the pores but also by increased pressure solution which is promoted by the clay between the quartz grains. No significant pores were observed under the microscope in sands with 6 percent or more argillaceous material. Kaolinite reduces porosity by forming books in pores but this kaolinite prevents quartz from growing. As some voids occur between the kaolinite books, there is less porosity reduction than with quartz growth.

Minerals which block or interfere with the formation of authigenic mineral cements, without significantly filling pores, will help in preserving porosity. Grain coatings are particularly effective in inhibiting quartz growth. Illite of detrital origin coated grains in some beds. Commonly the coatings were incomplete or very thin so that quartz growths were not blocked entirely but developed unique forms. Prismatic growths formed at sites on grains where coatings were absent or thin. Some of the grains with poorly developed coatings became overgrown and partially enveloped adjacent coated grains with no growths. This resulted in concave-convex contacts and eccentric growths (Heald and Larese, 1974). The limited growths indicate that sufficient silica was available for cementation and that coatings played a controlling part in restricting growth. In some porous zones, coatings were not visible but abnormal growths indicated that coatings had interfered with cementation and helped preserve porosity. The coatings in these zones either were too thin to be observed under the microscope or they were removed by later dissolution.

Mineral dissolution has created secondary porosity in some of the sandstone especially where good interstitial porosity allowed free circulation. In the sandstone that was tight because of argillaceous material or early carbonate cement, dissolution was at a minimum. Leaching of calcite occurred to some extent especially in the porous middle interval of the Bell well. The removed calcite was a secondary cement so the leaching reestablished some of the earlier porosity. The fairly numerous quartz grains with irregular margins might lead one to conclude that calcite leaching had been extensive. However, careful inspection of many of the irregular margins of the grains reveals traces of clay. Clay interferes with growth of quartz and typically produces irregular margins which could be mistaken for corrosion by carbonate that was later removed. Also the contact between feldspar and quartz are commonly irregular so that quartz has a corroded appearance where feldspar was later dissolved. Nevertheless, deep embayments into some of the detrital quartz grains indicate that some voids which presumably contained calcite were a result of calcite leaching which did increase porosity moderately.

Porosity was also increased by dissolution of phyllosilicates in quartz grains. Some of these voids are isolated in monocrystalline quartz but are connected with interstitial pores in many of the polycrystalline quartz grains. Some fine interstitial mica might have been removed but this would be difficult to detect. The various degrees of dissolution of feldspar also contributed to secondary porosity. However, feldspar content was low so that the maximum increase in porosity was only about 0.5 percent. The apparent dissolution of quartz also added slightly to the secondary porosity.

OVERVIEW OF POROSITY AND PERMEABILITY IN RELATION TO LITHOLOGY

Data from the Bell well illustrate the typical relationship between lithology of the Ravencliff sandstone and porosity and permeability. The variations in permeability, porosity and major lithologic features are shown in Figure 4. The lower part of the sand from 1186' to the base at 1202' formed under high energy conditions. The sand is medium to coarse grained with many pebbly layers. High flow is also indicated by low clay content and horizontal beds or cross bedding with slight inclination. The almost complete lack of porosity and permeability in the lower 7 feet of this zone is due to tight carbonate cement. From 1192' to 1194' the porosity was reduced by partial cementation by carbonate. However, this interval has some of the highest permeability because the carbonate occurs in isolated patches and flow is unimpeded in the coarse sand around the cemented patches. The low porosity and permeability

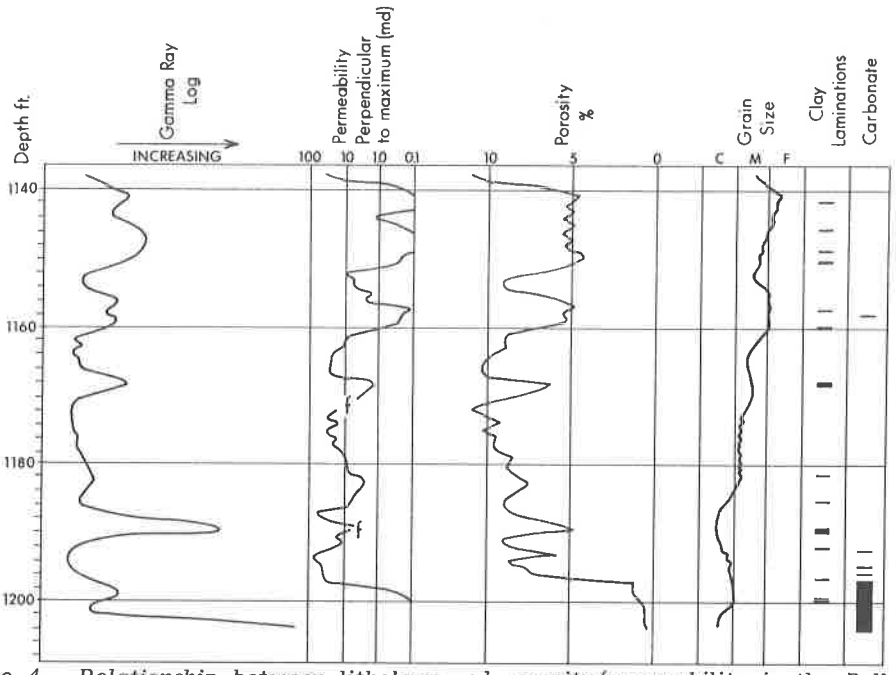

Figure 4. Relationship between lithology and porosity/permeability in the Bell well. Core depths adjusted to correspond to depths on gamma ray log. f indicates core was fractured on retrieval.

at 1188' - 1190' is due to shale clasts, and interstitial clay from disintegration of some of these clasts.

Most of the sand from 1153' to 1186' formed under a fairly high-flow regime as it is medium grained and low in clay. Quartz cement and pressure solution reduced porosity somewhat but the remaining porosity is relatively good with corresponding favorable permeability. At 1157' - 1160', 1168' - 1169' and 1182' - 1183, lower energy is indicated by closely spaced argillaceous laminations and interstitial clay. Porosity and permeability are low at these points because of the clay content and greater pressure solution promoted by the argillaceous material.

The upper part of a fining upward cycle occurs in the interval from 1141' - 1151'. The sand in this interval is finer, more argillaceous and has cross-bedding occurring in thin sets averaging 3 inches. Low flow regime is also indicated by thin clay laminae and more common lithic grains of shale, slate and fine-grained schist. The low initial porosity in this part of the sand was further reduced by greater pressure solution resulting from the more abundant clay. These factors produced an interval with low porosity and negligible permeability.

Many of the variations in rock characteristics are reflected in the gamma ray log (Fig. 4). Not all detailed variations in gamma radiation can be clearly related to obvious lithographic features but most of the argillaceous zones show increased radiation. The relatively thick interval of more argillaceous sand from 1141' - 1151' is well reflected in greater radiation shown in the gamma ray log. The rather sharp deflections at 1157' - 1160', 1168' - 1169', 1188' - 1190' and 1199' - 1200' are due to thin intervals of sand with closely spaced argillaceous laminations. Most of the lithologic changes indicated by the gamma ray log are reflected in variations in porosity and permeability (Fig. 4).

SUMMARY AND CONCLUSIONS

The submature to mature nature of the Ravencliff sandstone suggests a fluvial rather than marine environment of deposition. Additional support for a fluvial model of deposition is: 1) the presence of clay clasts, 2) steeply dipping unidirectional cross-

beds, 3) grain size fining upward, 4) erosional basal contact, 5) slight increase in quartz content with proposed flow direction and 6) lack of distinct marine indicators such as glauconite or shell fragments. Fining upward cycles, pebbly zones, and lack of abundant silt- and clay-sized particles, suggest that the Ravencliff sandstone is predominantly the product of a bed load stream in the study area.

Overall, the sand is relatively clean containing approximately 90 percent quartz, 3 percent authigenic carbonate, 3 percent detrital phyllosilicates (illite, etc.) and 2 percent authigenic kaolinite with small amounts of feldspar, heavy minerals and opaques. The Ravencliff sandstone initially had good porosity but a number of diagenetic processes considerably reduced the porosity. Quartz cement was significant in most of the sandstone except near the base, where calcite cement was important. A considerable part of the secondary quartz may have been furnish by pressure solution as solution appears to have occurred concurrently with much of the cementation. Some pores remained open because clay coatings prevented the nucleation of secondary growth on the host quartz. Small voids exist between kaolinite books which filled some pores and blocked quartz growth. Compaction attending pressure solution reduced porosity particularly in the illite-bearing parts of the sandstone. Mechanical compaction was also important in reducing porosity where appreciable numbers of ductile grains occurred.

Porosity was increased to some extent by diagenetic leaching. Moderate amounts of calcite cement were removed during the leaching. All stages in dissolution of feldspar were evident from slight corrosion to nearly complete removal of grains. However, less than 1 percent of the porosity was due to dissolution of feldspar because of the low feldspar content. Although phyllosilicates are generally stable, some inclusions of these minerals within detrital grains were leached, as evidenced by small voids in some of the quartz grains.

The highest porosity and permeability in the Ravencliff sandstone occurs in the coarser intervals of the sand where clay content is low, cementation and pressure solution are less complete, and circulation promoted the leaching of unstable components. These coarser intervals are more common in the lower part of the unit where deposition occurred under higher flow conditions.

ACKNOWLEDGMENTS

Thanks are extended to Floyd Wilcox for supplying samples and logs of the Ravencliff sandstone. Financial support from Appalachian Exploration and Development, Incorporated is gratefully acknowledged. The critical review of the manuscript by R. J. Diecchio is very much appreciated.

REFERENCES CITED

Donaldson, A. C., and Shumaker, R. C., 1979, Late Paleozoic molasse of Central Appalachians, *in* Donaldson, A. C., Presley, M. W., and Renton, J. J., eds., Carboniferous Coal Guidebook: West Virginia Geological and Economic Survey Bulletin B-37-3, p. 1-42.

Heald, M. T., and Larese, R. E., 1974, Influence of coatings on quartz cementation: Jour. Sed. Petrology, v. 44, p. 1269-1274.

Oliva, L. J., 1976, Petrographic factors affecting porosity in the Ravencliff sandstone of southern West Virginia [unpub. Masters problem report]: West Virginia University, 26 p.

Pawlowski, R. M., 1975, A petrologic study of the Ravencliff sandstone of southwestern West Virginia [unpub. Masters problem report]: West Virginia University, 20 p.

Pryor, W. A., 1960, Cretaceous sedimentation in Upper Mississippian embayment: Am. Assoc. Petroleum Geologists Bull., v. 44, p. 1473-1504.

Schalla, R. A., 1980, The Ravencliff of McDowell County, West Virginia: an Upper Mississippian delta complex: West Virginia Geological and Economic Survey, Eleventh Annual Appalachian Petroleum Geology Symposium, Abstracts with Program, Circular C-16, p. 33.

BAFERTISITE AND AN UNIDENTIFIED BaCaMnFeTi SILICATE FROM FOUNTAIN QUARRY, PITT COUNTY, NORTH CAROLINA

By

Richard L. Mauger
Department of Geology
East Carolina University
Greenville, NC 27834

ABSTRACT

Bafertisite, a rare BaFeMnTi-silicate, occurs in metamorphosed peralkalic granite and in post-deformational quartz veins in Fountain Quarry. This mineral is described from only three other localities in the world, one in Inner Mongolia and two in Siberia (USSR). The Fountain material has Mn/Mn+Fe=0.21; this ratio ranges from less than 0.10 in the Mongolian material to 0.48 in one of the Siberian samples. Fluorine (about one atom per formula unit) is probably essential. The powder pattern for the Fountain bafertisite is indexed with lowest $1/d^2$ residuals using orthorhombic symmetry and a=7.55, b=11.00 and c=5.40. These unit-cell data agree quite well with data cited in 1959 for the original Mongolian material. Monoclinic symmetry is cited in some later studies. A complex gray-brown BaCaMnFeTi-silicate occurs with bafertisite in the post-deformational quartz veins. The composition and X-ray data were not matched with any known phase or mixture of phases. Both minerals formed under low temperature, hydrothermal conditions following regional metamorphism of the granite.

INTRODUCTION

Two rare BaMnFeTi silicates were observed during the progress of a detailed petrologic study of the Fountain granite (Mauger and others, in press). One, a golden-yellow mineral, is identified as bafertisite. It was first described from Inner Mongolia, where it occurs with aegirine, fluorite, barite, and basnaesite in hydrothermal veins. Bafertisite has also been reported from two localities in the Soviet Union. The other is a gray-brown fibrous material that has not been identified.

GEOLOGIC SETTING AND GEOLOGY OF THE FOUNTAIN QUARRY

The Fountain Quarry is an isolated outcrop of crystalline rock that is completely surrounded by unconsolidated Plio-Pleistocene sedimentary strata (Snyder and Katrosh, 1979). Nearest crystalline exposures are 30 to 40 km to the west and northwest (Fig. 1). A foliated metamorphosed peralkalic granite, composed of albite, microcline, quartz, aegirine and NaFe-amphibole, is the major rock exposed in the quarry. This granite is cut by a few amphibolite (metabasalt) and metarhyolite dikes, and there are a few unmetamorphosed basalt dikes of probable Mesozoic age. There are two distinctive types of quartz veins in the quarry; both are very limited in occurrence. One type consists of medium-grained quartz with a few scattered, but very coarse-grained crystals of ilmenite and microcline. These are probably pegmatitic veins (now metamorphosed) that were injected as the granite was cooling following igneous crystallization. The other veins contain very coarse-grained quartz (>5 mm commonly) and a distinctive assemblage of minor phases including Mn-calcite, NaFe-amphibole, sphalerite, molybdenite, fluorite, bafertisite, and the gray-brown unknown. These veins also contain angular fragments of foliated granite. They probably formed after the major deformation and after the thermal metamorphic peak.

The granite is probably early Paleozoic (Cambrian), as determined by Rb/Sr isotopic studies (Mauger and others, in press). The alkali feldspars were completely recrystallized during a regional metamorphic event probably in the Hercynian or Acadian interval; however, an earlier Paleozoic age for the metamorphism (Ordovician) is possible. K-Ar ages on biotite and microcline indicate that the granite was cooling from 250°C to 200°C between 300 and 260 Ma ago, probably as the result of uplift.

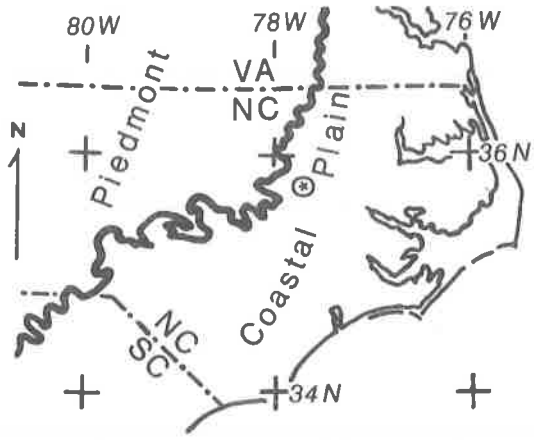

Figure 1. Index map showing the location of Fountain Quarry with respect to the Piedmont-Coastal Plain boundary. Fountain Quarry is marked by the oval with the star. The Piedmont-Coastal Plain boundary is shown by the very heavy black line.

BAFERTISITE

The first references to this mineral appeared (1959) in Chinese journals (Chi Jui, 1960; Semenov and Chang, 1960). Both articles contain exactly the same chemical and unit-cell data (Table 1). The original material came from the Baiyun-Obo region of Inner Mongolia. Two additional papers on bafertisite appeared in 1963 (Pang and Chen, 1964; Ya-Hsien and others, 1963). In both references, Semenov and Chang are given credit for discovering bafertisite; Chi Jui is not mentioned. The unit-cell data reported by Pang and Chen (Table 1) are fairly close to those given in the 1959 papers; however, the mineral was considered to be monoclinic and the a-axial dimension is slightly smaller than that given in the 1959 references. Pang and Chen proposed a different formula which includes OH(1-) sites and Si_2O_7 as the basic silicate unit (Table 1). Ya-Hsien and others, using material from Kazakhestan, also proposed monoclinic symmetry for bafertisite. However, their β-angle is much larger than that proposed by Pang and Chen (Table 1).

Ya-Hsien and others gave approximately doubled a- and c-axial dimensions as compared to those of earlier studies. They also proposed that bafertisite had a structure like that of a brittle mica in which Ba(2+) substituted for Ca(2+). This latter proposal is hard to justify since Si_2O_7 is not the basic phyllosilicate unit. Ganeev and others (1972) described a manganese and fluorine-bearing bafertisite from another locality (northern Baikal region) in the Soviet Union. Their fluorine analysis (3.50%) (Tables 1 and 3) is similar to that of the Fountain material (about one atom per formula unit); fluorine was not reported in earlier analyses (Table 1). Manganese occupied slightly less than one-half of the M(2+) sites in the Baikal material (Mn/Mn + Fe = 0.48). The Mn/Mn + Fe ratio is 0.21 in Fountain bafertisite and 0.1 or less in the Mongolian material. Niobium (Nb_2O_5) is reported in the Mongolian and Baikal materials (Table 3), and small, probably unessential quantities of Al, Ca, Mg, Sr, alkalies, and Cl may be present (Table 3). The preferred formula is $Ba(Fe,Mn)_2Ti(Si_2O_7)O(OH,F)_2$ and fluorine may be essential.

In later tabulations of mineralogic data, Roberts and others (1974) used the Pang and Chen unit-cell data, but the formula given in 1959 references was retained (Table 1). Berry (1980) gives the same cell dimensions and formula as the 1959 references (Table 1), and his portion of an indexed powder pattern was very helpful in identifying the Fountain material.

BAFERTISITE FROM FOUNTAIN

This mineral is a very sparse constituent of the granite. It is locally more abundant in the post-deformational quartz veins, but these were seen in only one

locality on the east wall of the passageway between the north and south pits. In the granite, bafertisite occurs as small highly acicular golden-yellow grains (<1 mm in length) (Fig. 2) that are typically associated with coarser-grained aegirine and NaFe-amphibole. The microprobe analyses were done on material in the granite. In the quartz veins the bafertisite occurs with sub-microscopic (1μ in diameter) anatase (Table 2) as stellate, almost fibrous clumps (<5 mm in length) that are localized along shear dislocations. This material was used for the x-ray studies. The yellow color

Table 1. Unit-cell data and formulas for bafertisite.

reference	a	b	c	β	F%	formula
(1)	7.55	10.98	5.36	**	nr	$BaFe_2TiSi_2O_9$
(2)	7.55	10.98	5.36	**	nr	same as (1)
(3)	6.80	10.98	5.36	94°	nr	$BaFeFeTi(Si_2O_7)O(OH)_2$
(4)	6.82*	10.60	6.24*	119°30'	nr	same as (3)
(5)	--	--	--	--	3.50	$Ba(Fe,Mn)_2Ti(Si_2O_7)$ (O,OH,F)
(6)	6.80	10.98	5.36	94°	nr	same as (1)
(7)	7.55	10.98	5.36	**	nr	same as (1)
(8)	7.56	11.00	5.40	**	3.51	$Ba(Fe,Mn)_2Ti(Si_2O_7)O(OH,F)_2$

* one-half quoted value
** orthorhombic or monoclinic with β near 90°

References:

(1) Chi Jui (1960)
(2) Semenov and Chang (1960)
(3) Pang and Chen (1964)
(4) Ya-Hsien and others (1963)
(5) Ganzeev and others (1972)
(6) Roberts and others (1974)
(7) Berry (1980)
(8) this paper

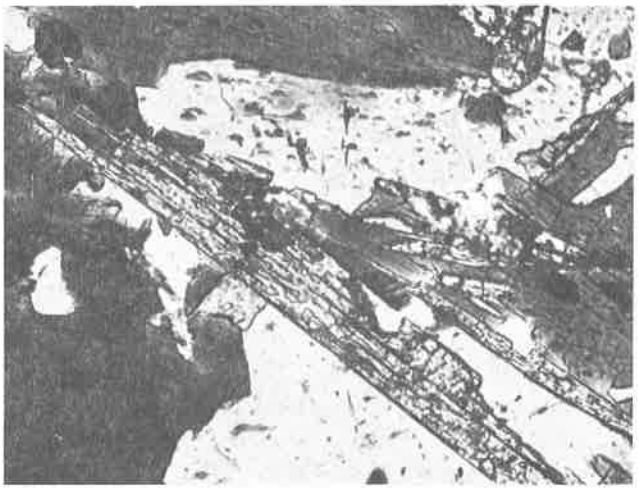

Figure 2. Photomicrograph of bafertisite in Fountain granite. Long dimension of photo represents 0.3 mm. Mottled light-gray acicular grains are bafertisite. Note the prominent cleavage. Light-colored grains are albite and quartz. Dark grains are aegirine and NaFe-amphibole. Black grains are magnetite.

Table 2. X-ray diffraction data for Mongolian and Fountain bafertisite.

Diffraction Data				Unit-Cell Dimensions			
*d	d	*I	*hkl		Mong	Fount	hkl
nl	5.40	vs	[001]	a	7.55	7.56	300
nl	3.63	s	[030]?	b	10.98	11.00	040
(3.52)	(3.52)	s	(anatase 101)	c	5.36	5.40	002,221
nl	3.43	s	[121]				
nl	3.11	w	[220]				
nl	2.82	s	[131]				
2.77	2.75	s	040				
2.71	2.70	vs	221;[002]				
2.65	absent		002				
2.52	2.52	m	300, 102				
(2.38)	(2.39)	m	(anatase 004)				
2.23	2.21	m	240,311,[202]				
2.17	2.17	s	032				
2.11	2.11	w	150, 321				
2.07	2.07	w	330				
(1.89)	(1.90)	w	(anatase 200)				
1.75	1.75	w	411,[103]				
1.70	1.70	w	broad; (includes anatase 105)				

*d Mongolian bafertisite: nl, not listed; parentheses indicate d values for anatase; brackets indicate indices based on c=5.40.
d Fountain material.
*I Intensities strongly affected by preferred orientation; w(weak), m(moderate), s(strong), and vs(very strong).
*hkl Indices without brackets from Berry (1980).

Table 3. Chemical analyses of bafertisite from Fountain and from other localities.

	1	2	3	4	5
SiO_2	23.81	23.94	23.88	23.68	25.18
TiO_2	15.10	15.35	15.23	15.39	14.27
Al_2O_3	0.09	0.03	0.06	0.29	1.00
FeO	21.93*	22.33*	22.13*	22.56	10.82
Fe_2O_3	—	—	—	1.08	3.67
MnO	6.11	5.72	5.92	1.62	12.77
MgO	0.12	0.10	0.11	0.50	0.10
CaO	0.24	0.15	0.20	0.37	0.30
Na_2O	0.19	0.05	0.12	0.49	0.38
K_2O	0.16	0.17	0.17	0.12	0.33
BaO	30.77	30.24	30.51	29.98	26.59
SrO	0.40	0.10	0.25	tr	nr
Nb_2O_5	nr	nr	nr	0.84	0.32
F	3.46	3.56	3.51	nr	3.50
H_2O+	nr	nr	nr	1.65	2.16
Cl	0.02	0.03	0.03	0.63	nr
SO_2	0.15	0.12	0.14	nr	nr
Sum	102.55	101.89	102.22	**97.20	101.29

* total iron as FeO
** does not include 1.14% H_2O-
columns 1 and 2 - from Fountain by microprobe
column 3 - average of columns 1 and 2
column 4 - from Inner Mongolia (Semenov and Chang, 1960; Chi Jui, 1960)
column 5 - from Baikal region, USSR (Ganeev and others, 1972)
empirical formula for Fountain material - $Ba(Fe,Mn)_2TiSi_2F[O_{8.5}]$
tr - trace; nr - not reported

darkens slightly following initial exposure; some grains in the granite are red and appear to be oxidized. Identification is based on x-ray and chemical similarities (Tables 2 and 3) with the Mongolian material. Incomplete optical data (Table 4) for the Fountain bafertisite generally agree with data for the Mongolian bafertisite (Berry, 1980; Roberts and others, 1974).

The orthorhombic unit-cell data cited in the original 1959 references (Berry, 1980) were used for indexing the powder pattern of the Fountain material, except that c=5.40 gave slightly better results than c=5.36. All lines were indexed (Table 3) and $1/d^2$ residuals ($\bar{R}$=0.0007) were quite small. Inclusion of a β-angle (monoclinic symmetry) and/or use of an a-axial dimension other than 7.56 resulted in much larger residuals and in some lines not being indexed. The Fountain material shows d=2.70 as the most intense reflection, and it has no d=2.65 reflection which is listed (Berry, 1980) as the most intense reflection in the Mongolian material (Table 2). The discrepancy is not due to an error in the goniometer setting because anatase reflections (Table 2) on the Fountain chart give d-spacings that are within 0.01 of the accepted values (JCPDS Data Book, 1980). If the d=2.70 Fountain reflection is really 002, then the very strong reflection d=5.40 is 001 and the c-axial dimension is 5.40. Perhaps the d=2.65 reflection in the Mongolian pattern was caused by another mineral in the sample.

UNIDENTIFIED GRAY-BROWN MINERAL FROM FOUNTAIN

This material was seen only on shear surfaces in the post-deformational quartz veins. Freshly exposed material is brownish gray with a silvery-pink hue. The color darkens considerably with time, and the powder color for the darkened material is a rich chocolate brown. The gray-brown unknown has a strongly fibrous habit, and it has the same associated minerals as bafertisite.

The x-ray and chemical data (Table 5) were not matched with those of any known mineral. The optical characteristics (Table 6) and the chemical analysis have some similarities to those of bafertisite. The possible empirical formula (Table 5) is fairly complex. Minor elements include As, La, Y, Rb, Zr, Sr, B and Be. Since all but one percent of the analysis is accounted for, major revision in or additions to the composition are unlikely. The gray-brown material appears to be a single phase when observed in refractive index oils. Microprobe analyses of the fibers gave similar results, suggesting that any intergrowth of phases would have to be on a submicroscopic scale. The quartz indicated in the x-ray data (Table 5) has been verified by optical examination of the powdered material. A few grains of NaFe-amphibole

Table 4. Optical data for Fountain bafertisite.

Refractive indices (grains resting on cleavage surfaces)
- 1.85 to 1.86; ray vibrates parallel to long dimensions of grain
- 1.81 to 1.82; ray vibrates perpendicular to long dimension of grain

Extinction
- Parallel with long dimension of acicular fragments

Pleochroism
- Grains resting on cleavage; both rays are light-golden yellow
- Grains with cleavage at steep angle to thin-section; slower ray is golden yelow, faster ray is light-golden yellow

Sign, 2V (based on poor bisetrix figure)
- Biaxial negative; 2V is intermediate

Birefringence
- Maximum colors in thin-section are low to middle second order; however, birefringence may be higher because grains with Y perpendicular to stage may not have been observed

Cleavage-optical orientation
- There is one perfect cleavage (at least)
- X may be perpendicular to that cleavage

Bafertisite (Mongolia)
- α 1.808, γ 1.860; biaxial negative, 2V is 54°; one distinct cleavage, one poor cleavage; occurs as aggregates of acicular crystals; red, yellowish red, or light brown

Table 5. X-ray and chemical data, Fountain gray-brown unknown.

Diffraction Data

d	*I	Remarks
17.1	s	
11.4	vs	dominant peak
8.31	m	
5.75	w	one-half d=11.4
4.53	w	
4.21	w	201 max microcline
3.84	w	one-third d=11.4
3.33	m	101 quartz d=3.34
3.27	m	max microcline
3.09	w	
3.02	w	
2.87	m	one-fourth d=11.4
2.27	w	
2.55	w	broad
2.08	w	
1.98	w	
1.75	w	
1.66	w	
1.56	w	

Chemical Analysis

		*	**
SiO_2	35.00	0.5825	11.14
TiO_2	9.55	0.1195	2.28
Al_2O_3	1.57	0.0308	0.59
*FeO	30.48	0.4242	8.11
MnO	6.99	0.0985	1.89
MgO	0.51	0.0127	0.24
CaO	2.91	0.0519	0.99
Na_2O	1.02	0.0329	0.63
K_2O	0.96	0.0204	0.39
F^2	0.94	0.0495	0.95
BaO	4.31	0.0281	0.54
*LOI	4.67	0.2594	4.96
Sum	98.91		

* moles per 100 grams
** atoms per Fe+Mn = 10
*FeO total iron as FeO
*LOI lost on ignition at 1000°C; assumed to be OH or H_2O

*I Intensities strongly affected by preferred orientation; w(weak) m(moderate), s(strong), vs(very strong)

Emission Spectrographic Data (ppm)

As	500	Nb	300	Zr	500	Mo	< 2
B	200	Pb	10	*Bi	<10	Ni	< 5
Be	100	Sn	100	Cd	<50	Sb	<100
Cu	30	Sr	1000	Co	< 5	Sc	< 10
Ga	15	W	50	Cr	<10	V	< 10
La	500	Y	1500	Ge	< 20	Zn	< 200

* number following < symbol indicates detection limit

were also observed; however, these were far too sparse (<0.1%) to show up in the x-ray pattern. Microcline indicated in the x-ray data (Table 5) was not positively identified in the grain mounts; however, it is a common constituent of the granite and quartz veins. The strong peak at d=17.1 was considered as possibly due to ashcroftine, but absence of other peaks and the chemical composition (Table 5) argue against this possibility. The refractive indices (1.54) of ashcroftine are also much lower than those of the gray-brown unknown (Table 6). The x-ray pattern also has some similarities to that of murmanite. Thus the gray-brown material may be a complex mixture or it may be a single phase that has not been described as yet.

CONDITIONS OF FORMATION

The bafertisite and the gray-brown unknown formed under green schist-grade metamorphic conditions. The high purity of the alkali feldspars in the granite and mineral assemblages in the amphibolites indicate that peak metamorphic temperatures (500°C?) were followed by a prolonged cooling period, during which the feldspars continued to equilibrate to fairly low temperatures (200°C or so). Recrystallization of an original alkali feldspar and titanomagnetite in the granite released Ba and Ti and made them available for incorporation into minor phases. Mn and Fe occur in late-stage veins in such phases as spessartine-andradite garnet and ferropargasite. Calcite, widely distributed in the quarry, has small but persistent Mn and Fe components. A

Table 6. Optical data for Fountain gray-brown material.

Refractive indices
- 1.75 to 1.76; Z is parallel with long dimension of fibers
- 1.72 to 1.73; Y is perpendicular with long dimension of fibers

Extinction
- Parallel with long fiber dimension

Pleochroism
- Z is dark-yellow brown
- Y is light-yellow brown

Sign, 2V, optical-crystallographic orientation
- Biaxial negative, 2V is about 70°; probably orthorhombic
- X is perpendicular to the flattened fiber aggregates

Birefringence
- Low to middle second order colors for grains perpendicular to X

Cleavage
- Probably at least one perfect cleavage; interpretation complicated by fibrous habit

few carbonate grains are Mn- and/or Fe-rich. Fluorite occurs as a minor phase in the granite and in the late-stage veins. These constituents and others which were not readily accepted into common rock-forming minerals formed the BaMnFeTi silicates under low-temperature (200-300°C) hydrothermal conditions following the main metamorphic event.

ACKNOWLEDGMENTS

Dr. Todd Solberg, director of the micropobe facility at Virginia Polytechnic and State University, helped the author with the microprobe analyses, and John S. White, Jr., of Smithsonian Institution identified the anatase in the bafertisite goniometer chart. I wish to thank Dr. Richard Mitchell for his comments and for pointing out some additional literature citations for bafertisite. Martin Marietta Corporation kindly allowed the author access to the Fountain Quarry. The study was aided by a small grant from the East Carolina University Research Council.

REFERENCES

Berry, L. G., 1980, X-ray intensity and indexing data for bafertisite; card 14-541 in Mineral Powder Diffraction File (Data Book), Internat. Centre for Diffraction Data (Swarthmore, PA), p. 66.

Chi Jui, Peng, 1960, The discovery of several new minerals of rare elements: Amer. Mineralogist, v. 45, p. 754. (abstract of original 1959 article in Chinese).

Ganeev, A. A., Efimov, A. F., and Lyubomilova, G. V., 1972, Manganiferous bafertisite from the Burpala massif (northern Baikal): Amer. Mineralogist, v. 57, p. 1005 (summary of a 1971 paper in Russian).

Mauger, R. L., Spruill, R. K., Christopher, M. T., and Shafiqullah, M., (in press): Petrology and geochronology of peralkalic metagranite and metarhyolite dikes, Fountain Quarry, Pitt County, North Carolina: submitted to Southeastern Geology.

Pang, Chih-Chung and Shen, Chin-Chuan, 1964, Crystal structure of bafertisite: Chemical Abstracts, v. 60, p. 76 (abstract of a 1963 article in Chinese in a Chinese journal).

Roberts, W. L., Rapp, G. R., Jr., and Weber, J., 1974, Encyclopedia of Minerals: Van Nostrand Reinhold Co., New York, New York, p. 47.

Semenov, E. I., and Cheng, Pei Shan, 1960, New mineral: bafertisite: Chemical Abstracts, v. 54, p. 13996 (abstract of a 1959 article, in Russian, in a Chinese journal).

Snyder, S. W., and Katrosh, M. R., 1979, An exposure of marginal marine Pleistocene sediments, Pitt County, North Carolina: Southeastern Geology, v. 20, p. 247-259.

Ya-Hsien, K., Simonov, V. I., and Belov, N. V., 1963, Crystal structure of bafertisite: Chemical Abstracts, v. 59, p. 3386-3387 (original article in Russian, in Dokl. Akad. Nauk SSSR, v. 149, p. 1416-1419, 1963).

OLIGOPYGOID ECHINOIDS AND THE BIOSTRATIGRAPHY OF THE OCALA LIMESTONE OF PENINSULAR FLORIDA

By

Michael L. McKinney
Department of Geology and Geophysics
Yale University
New Haven, Connecticut 06511

And

Douglas S. Jones
Department of Geology
University of Florida
Gainesville, Florida 32611

ABSTRACT

The Upper Eocene Ocala Limestone of peninsular Florida is characterized by a three-species, successional lineage of oligopygoid echinoids which form the basis of the most useful biozonation scheme for this important unit. A biometric analysis of all three species indicates that the important species-diagnostic traits, periproct position and peristome roundness, underwent only minor change during ontogeny. The data also indicate that the traits within one species, *Oligopygus haldemani*, exhibit no directional change through time and that species transitions (biozone boundaries) are abrupt. These observations suggest there is little chance of species misidentification due to ontogenetic or phylogenetic effects when using this lineage for biostratigraphic purposes.

INTRODUCTION

Background

The Ocala Limestone, of Late Eocene age, is one of north Florida's most widespread and prominent geologic units. Where it crops out (see Fig. 1), it serves as an important source of lime rock which is commonly used by the building and road construction industries. Where it occurs below the surface, it is usually a major constituent of the Floridan aquiefer system. In thickness, the Ocala Limestone often dominates much of the stratigraphic column. It is also one of the most studied units in Florida (e.g., Cooke, 1915; Puri, 1957; Puri and Vernon, 1964; and Chen, 1965). Yet, despite its significance, the stratigraphy of the Ocala Limestone itself remains ambiguous and difficult to apply in the field.

The most widely used stratigraphic scheme for the Ocala Limestone is that proposed by Puri (1957) which is summarized as follows:

Jackson Stage
Ocala Group (Upper Eocene)
Crystal River Formation
Williston Formation
Inglis Formation

This scheme raises the Ocala Limestone to group status and gives the appearance of subdividing the group into three lithostratigraphic units or formations. Yet most field geologists find it very difficult to distinguish these units on a lithologic basis, especially when they appear in outcrop. Puri (1957) distinguished these units primarily on the basis of benthic foraminifera and select associated invertebrate fossils. Thus, according to the American Commission on Stratigraphic Nomenclature (1961), these are not true lithostratigraphic units but are in fact biostratigraphic units. Terminology aside, this scheme presents another problem to the field geologist by its usage of benthic foraminifera and other microfauna as the basic zonation criteria. Proper

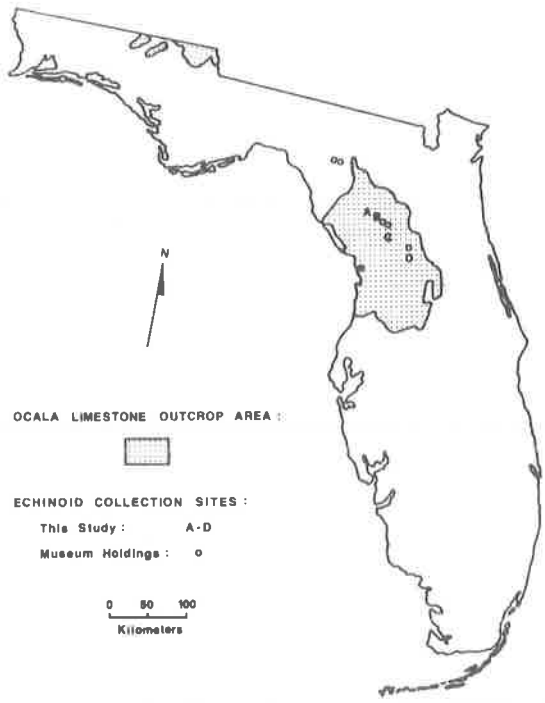

Figure 1. Outcrop area of the Ocala Limestone in Florida with the locations of echinoid collection sites.

species identification of these organisms is often difficult due to their small size, poor preservation, and the fact that they are usually encrusted with calcium carbonate.

In view of the above considerations, it is not surprising that a number of attempts have been made to zone the Ocala Limestone in other ways, especially by the use of larger, more easily recognizable organisms. For example, bryozoans (Cheetham, 1963) and bivalves (McCullough, 1969) have both been used. However, these attempts at zonation have not been entirely successful. The organisms involved are limited in terms of their lateral and/or vertical distribution in the Ocala Limestone as well as in abundance. There is one group of organisms, however, which does seem to provide a satisfactory zonation of the Ocala Limestone--the irregular echinoids.

Oligopygoid Echinoids of the Ocala Limestone

Approximately 32 species of irregular echinoids are recognized in the diverse fauna of the Ocala Limestone (Croft, 1980). Of these, only a few are very abundant. Three of the most abundant species belong to the genus *Oligopygus*. They range throughout the Ocala Limestone and are areally quite widespread. Thus, it was upon this group, the oligopygoids, that Zachos and Shaak (1978) focused in creating their echinoid biozonation scheme for the Ocala Limestone, a system which probably represents the most useful zonation of this unit yet proposed (McKinney and Jones, 1982).

As seen in Figure 2, the three common species of oligopygoids provide essentially exclusive (non-overlapping) range zones in the Ocala Limestone. *O. phelani* Kier occupies the lowermost range zone followed by *O. haldemani* (Conrad) and *O. wetherbyi* de Loriol, respectively. In terms of the Puri (1957) scheme discussed above, the *O. phelani* biozone is co-extensive with the Inglis "Formation", the *O. haldemani* biozone with the Williston "Formation" and the lower part (amount uncertain as of now) of the Crystal River "Formation", and the *O. wetherbyi* biozone with the remainder of the Crystal River "Formation" (see Fig. 2). The overlap between these biozones is minimal, rarely, if ever, exceeding 1 m.

Period:	Tertiary		
Epoch:	Late Eocene		
Stage:	Jackson		
Group:	Ocala Limestone		
Formation:	Inglis	Williston	Crystal River
Oligopygoid Biozonation:		O. phelani	O. haldemani
		O. wetherbyi	

Figure 2. Oligopygoid echinoid biozonation scheme for the Ocala Limestone, modified from Zachos and Shaak (1978).

In addition to their abundance, widespread distribution, and fairly exclusive range zones, easy recognition of the oligopygoids is another favorable feature for their use in biozonation. All three species in the Ocala Limestone can be distinguished on the basis of only two species-diagnostic traits: peristome roundness and periproct position. As illustrated in Figure 3, *O. phelani* is the only one of the three species with a circular peristomal depression. *O. haldemani* and *O. wetherbyi* are both characterized by a laterally ovate depression. *O. haldemani* and *O. wetherbyi* can be differentiated from each other by the fact that the latter has a periproct which is located about halfway between the posterior margin and the peristome. In contrast, *O. phelani* and *O. haldemani* both have an inframarginal periproct. Figure 4 further illustrates these distinguishing features. In addition to these species-diagnostic traits, the three species vary in their overall mean size. Kier (1967) reports a mean length of 11 mm for *O. phelani*, 21 mm for *O. haldemani*, and 36 mm for *O. wetherbyi*. However, length is not a clear-cut species-diagnostic trait since there is considerable overlap between the species (McKinney, 1982).

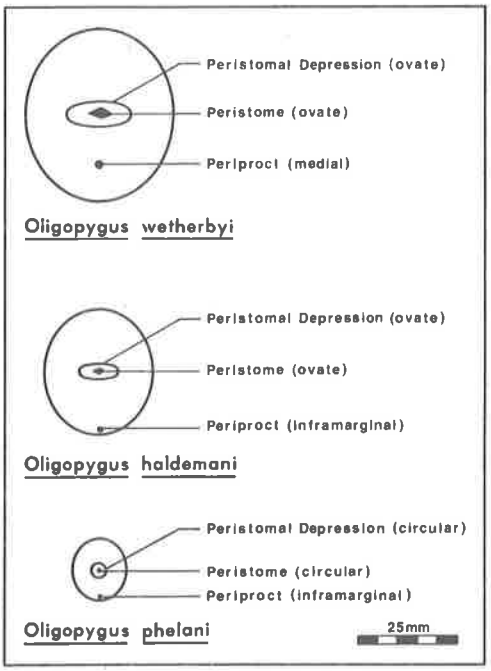

Figure 3. The major species-diagnostic traits of the three oligopygoid echinoid species of the Ocala Limestone are compared in this schematic view of their oral surfaces (after Croft, 1980).

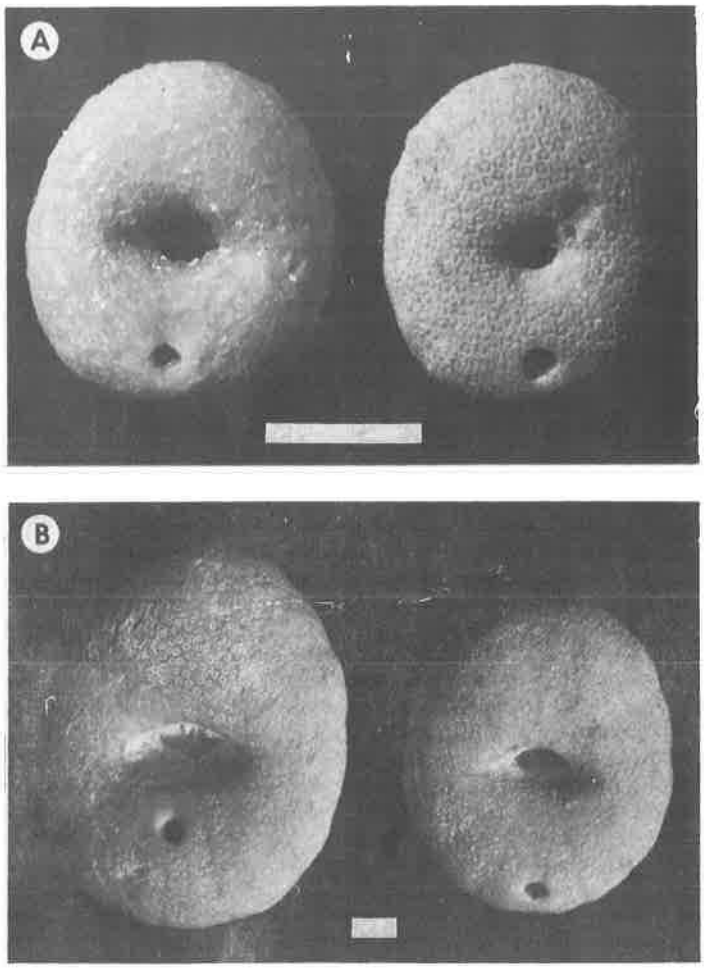

Figure 4. Photographs of the oral surfaces of the three oligopygoid species. A. O. haldemani *(left, recrystallized) with ovate peristome and inframarginal periproct and* O. phelani *(right) with circular peristome and inframarginal periproct. B.* O. wetherbyi *(left) with ovate peristome and medial periproct and* O. haldemani *(right) with ovate peristome and inframarginal periproct. Scale bar lengths represent 5 mm.*

Purpose

In light of the above discussion, it holds that the more complete an understanding we have of variation in this important group of echinoids, the more confidently and accurately we can use them as zonal markers. Since the entire Order Oligopygoida has been extinct since the Late Eocene (Kier, 1967), any understanding of them must come largely from their fossil record. The most important aspects of these organisms relevant to the biostratigraphy of the Ocala Limestone relate to variation of their species-diagnostic traits: peristome roundness and periproct position. Specifically, two items need to be learned. During ontogeny, was there any change in either of these traits? If so, then the juvenile of one species may closely resemble the adult of another. For example, if the periproct of *O. wetherbyi* were to migrate toward the peristome during growth, then a juvenile's test may be of similar size and have a periproct position similar to that of an adult *O. haldemani*.

Another item to be learned relates to phylogeny. Specifically, what is the relationship of these species to one another? If this is an evolutionary lineage with each species evolving into the succeeding one, we need to know whether or not forms

with intermediate species-diagnostic traits exist at or near the transition horizon between species. If so, proper identification may be difficult. Alternately, these species may represent a succession of related, geographically adjacent forms. In this case, each biozone represents a species which supplanted the preceding one. It seems likely that this sort of migration would be stimulated by environmental change, such as a change in water depth. If the oligopygoids do indeed represent such an "ecological" succession, then they are best understood as such and the transition zones should be examined for evidence. This does not remove the possibility that evolution may have occurred during the period that each species was in the area.

This study was undertaken for the purpose of answering these questions. Specifically we sought to: 1) look for change in the species-diagnostic traits during individual growth (ontogeny), and 2) examine the phylogenetic relationships between these species by looking for intermediate morphs and analyzing morphological change in one species (*O. haldemani*) through time.

MATERIALS AND METHODS

This study analyzed specimens of fossil oligopygoids collected by the senior author as well as specimens in the Florida State Museum, University of Florida, Gainesville, Florida. The field collecting was done in four limerock quarries (A-D) whose locations are shown in Figure 1. In addition, six sites were represented by specimens from the museum collections (also see Fig. 1). The precise locations for all ten sites are given in McKinney (1982).

Fieldwork consisted not only of collecting large numbers of loose and dislodged specimens from the quarry floors, but also recording the relative stratigraphic positions of 135 specimens of *O. haldemani* by measuring their height above the relatively flat quarry floors. In situ measurements were possible in all but Quarry D (Fig. 1).

Upon return to the laboratory, all specimens were cleaned with a 5 percent solution of hydrochloric acid. Measurements of various morphological parameters were then made using a dial-faced caliper. These measurements provide a way of quantitatively describing each individual echinoid test. A total of 12 parameters were measured in each individual (McKinney, 1982) but only the following are discussed here: 1) Test Length--greatest distance between the anterior and posterior poles of the ambitus. Test length was used as the basic indicator of an individual's size. 2) Periproct Position--the position of the periproct relative to the posterior margin and the peristome. This trait was quantified by dividing the peristome-periproct distance by the peristome-posterior margin distance. Thus,

$$\text{Periproct Position} = \frac{\text{Peristome-Peripoct Distance}}{\text{Peristome-Posterior Margin Distance}}$$

The closer value is to 1, the more marginal is the periproct. 3) Peristome Roundness--expresses the "circularity" of the peristome (or, more accurately, peristomal depression). This trait was quantitatively described by dividing peristome length by peristome width. Thus,

$$\text{Peristome Roundness} = \frac{\text{Peristome Length}}{\text{Peristome Width}}$$

The closer this value is to 1, the more circular is the peristome.

A total of 1113 individual specimens were measured for the above parameters (McKinney, 1982). The data were stored on cards for computer-assisted analysis at the Northeast Regional Data Center, University of Florida. A complete analysis was then carried out using a SAS program (SAS, 1980) which generated not only thorough descriptive data for each species with regard to the species-diagnostic traits, but produced correlation coefficients as well (McKinney, 1982).

RESULTS AND DISCUSSION

Ontogenetic Effects on Species-Diagnostic Traits

By analyzing a large number of fossil tests over the widest size range available, it is possible to obtain some idea of the ontogenetic development of a particular oligopygoid species. Assuming that different test sizes (that is, lengths) within the same species represent different stages of growth, then a growth sequence can be constructed in which relative or absolute change in the species-diagnostic traits can be observed. One of the best methods to observe this change is by correlation analysis of the traits. A significant correlation between test length and the species-diagnostic trait (either periproct position or peristome roundness) would indicate that the trait underwent some sort of consistent and uniform change during the growth of the organism (that is, as test length changed, so did the trait).

The results of such an analysis are shown in Table 1. Looking first at periproct position, it is evident that *O. phelani*, having the highest coefficent, shows a pronounced ontogenetic effect on this trait. However, since periproct position is not the distinguishing trait for *O. phelani* (it is peristome roundness), the apparent migration of the periproct throughout ontogeny poses no major problems. *O. haldemani* shows no correlation while *O. wetherbyi* exhibits a weak correlation that is barely significant at the 5 percent level. The negative value of all three indicates an inverse relationship between the variables as shown in Figure 5. Thus, we see a general migration of the periproct away from the margin in *O. phelani* as it developed, a much

Table 1. Correlation coefficients (r) with 5 percent significance levels for the two major species-diagnostic traits, periproct position and peristome roundness, and length in the three oligopygoid species. N corresponds to the sample size.

	Periproct Position	Peristome Roundness
O. phelani--length	-0.58; ± 0.13 (N=220)	0.21; ± 0.14 (N=193)
O. haldemani—length	-0.00; ± 0.08 (N=726)	0.11; ± 0.08 (N=642)
O. wetherbyi--length	-0.20; ± 0.19 (N=112)	0.00; ± 0.20 (N=96)

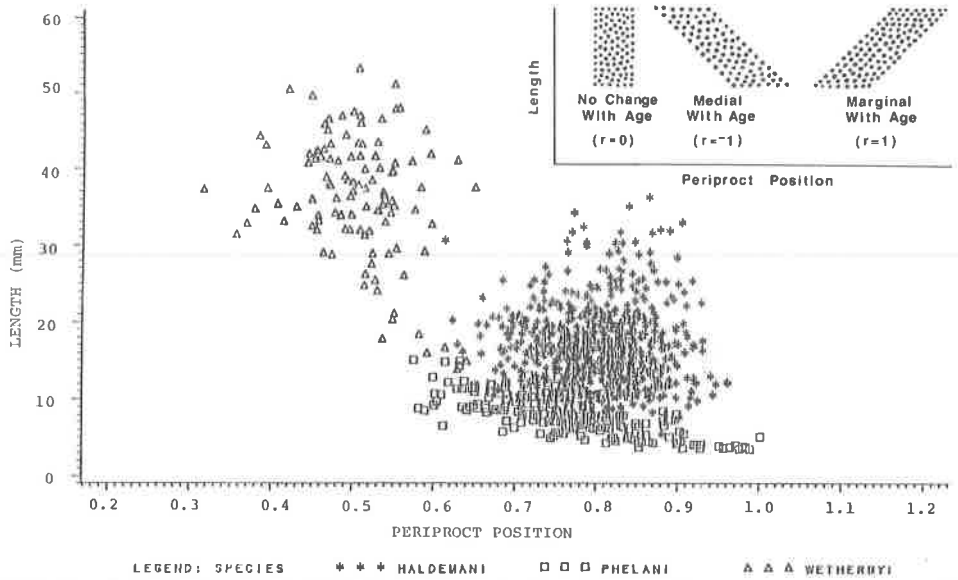

Figure 5. Length versus periproct position (defined in text) scatter diagram of 1113 specimens representing all three oligopygoid species. Trends in the arrangement of these data clusters, as illustrated by the "ideal" patterns shown in the inset, indicate whether or not the periproct migrated throughout ontogeny, that is as length (which is used as a measure of size and thus, age) increased.

weaker trend toward migration in *O. wetherbyi*, and no migration at all in *O. haldemani*. These relationships are more easily visualized when they are compared to the "ideal" patterns shown on the inset of Figure 5. Both the "ideal" and the "real" point patterns exhibit a rather broad horizontal component due to the considerable amount of individual variation within each species.

The values for peristome roundness in Table 1 and Figure 6 likewise reveal a mixed pattern of relationships. Both *O. phelani* and *O. haldemani* show a very weak but significant relationship. As length increases, the peristome tends to become slightly more ovate in both. However, as can be seen from the inset of "ideal" patterns in Figure 6, these trends are quite minor and the overall configuration is one of little change in this trait during growth. The data for *O. wetherbyi* indicate no correlation exists.

Phylogenetic Effects on Species-Diagnostic Traits

Long term trends in the species-diagnostic traits were assessed in two ways. For those specimens for which stratigraphic control was available, an attempt was made to observe the change directly. Figure 7A shows the results of this analysis for periproct position. Take note that no attempt was made to stratigraphically correlate the 3 quarries shown. For each height interval, the mean and range of test lengths for the 10 individuals within it are shown. As can be seen, there is no indication of directional change in the periproct position of *O. haldemani* through time. Rather, what minor change there was remained quite random. This is characteristic of all three quarries, though the best-documented is Quarry B (Fig. 1). Figure 7B shows that for the species-diagnostic trait peristome roundness, there was again no overall directional trend. Here, too, the change was rather minor though perhaps not so random. However, since peristome roundness is not the distinguishing feature of *O. haldemani*, this does not affect species recognition. The fact that juveniles as well as adults were averaged

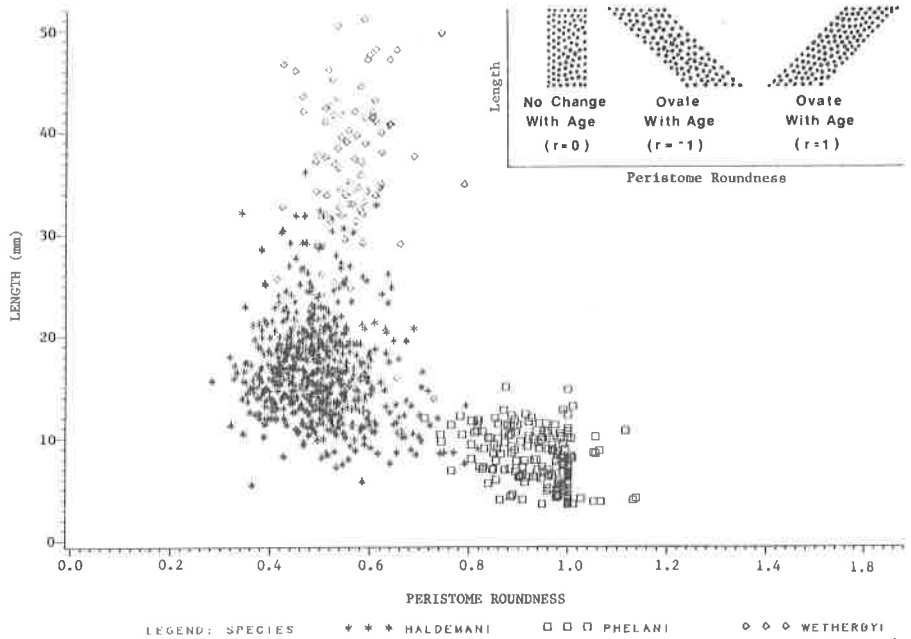

Figure 6. Length versus peristome roundness (defined in text) scatter diagram of 1113 specimens representing all three oligopygoid species. Trends in the arrangement of these data clusters, as illustrated by "ideal" patterns shown in the inset, indicate whether or not the shape of the peristome changed throughout ontogeny, that is as length (which is used as a measure of size and thus, age) increased.

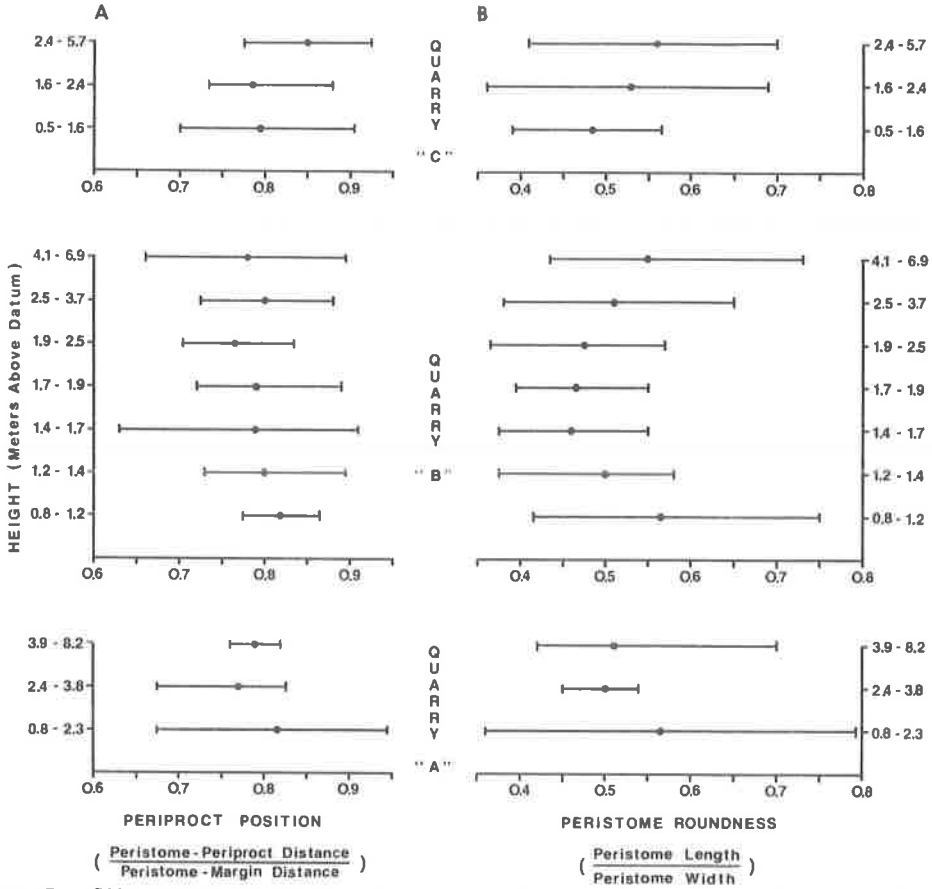

Figure 7. Oligopygoid specimens collected in situ *from the walls of three quarries (A, B, C--see Fig. 1) were used to assess changes over time. Ten individuals from various heights above datum (quarry floor) defined each stratigraphic interval. The mean and range of values for each interval in each quarry are shown for A. Periproct Position and B. Peristome Roundness. The relative stratigraphic position of the three quarries to one another is undetermined.*

together (ontogenetic mixing) does not contribute to the random patterns here since, as the preceding section shows, little ontogenetic change in these traits occurred in this species.

Another means of observing change in the species-diagnostic traits (though more indirectly) was by the use of an additional scatter diagram. By simultaneously comparing the periproct position and peristome roundness of all 1113 specimens, it was possible to search for intermediate morphs between the three species. As can be seen in Figure 8, the species are separated into three fairly discrete clusters. More importantly, this graph shows the presence of few intermediate forms. That is, very few specimens of one species are found within the cluster of either one of the other two. Quantitatively, only two *O. haldemani* tests (0.3% of the total number measured) fell within the boundaries of the *O. wetherbyi* cluster. Conversely, only six individuals of *O. haldemani* (0.9% of the total) are found within the boundary of the *O. phelani* cluster (the "intermediate" individuals are identified by their stratigraphic provenance). There is no overlap at all between the *O. phelani* and *O. wetherbyi* clusters. This lack of overlap between the three species indicates that the species transitions in this lineage occurred quite abruptly in the Late Eocene deposits of peninsular Florida. Thus, if this succession represents an evolutionary lineage (that is, they represent chronospecies), then it can be said that evolution here did not occur in a gradual step-

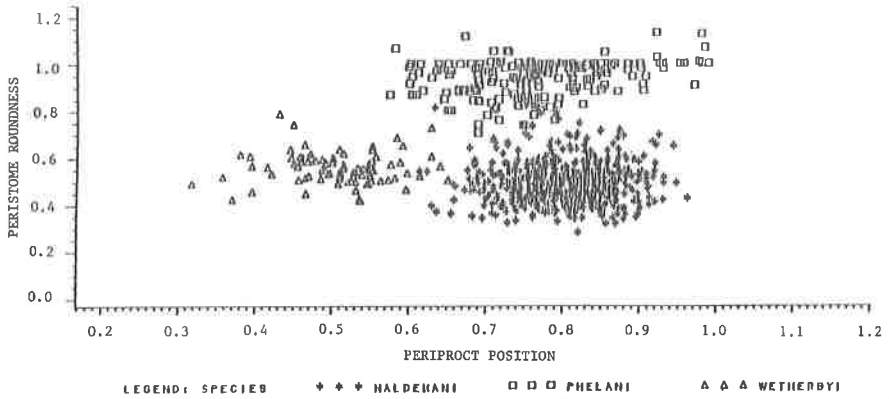

Figure 8. Simultaneous comparison of periproct position and peristome roundess in all 1113 specimens of oligopygoid echinoids to search for intermediate morphs.

by-step fashion. Rather, the speciation events were quite rapid in terms of geologic time, presumably by some allopatric mode. Alternately, this succession may represent an ecological succession in which case each abrupt change in species represents the migration into the area of an adjacent, related species of oligopygoid and its replacement of the preceding species. This migration would probably be stimulated by some type of environmental change. This latter alternative is suggested by the fact that the carbonate particle size may be somewhat finer in the rocks of the central biozone (*O. haldemani*) indicating a lower-energy environment of deposition than in the two other biozones (Croft, 1980). However, whichever explanation is correct, the fact is that for stratigraphic purposes, the species transitions are quite abrupt in the study area of northern Florida.

CONCLUSIONS

The results of this study indicate that the three species of oligopygoid echinoids used in the biozonation of the Ocala Limestone are even better index fossils than previously thought. A biometric analysis reveals that while using the two species-diagnostic traits, periproct position and peristome roundness, there is little chance of misidentification due to either ontogenetic or phylogenetic effects.

In the case of periproct position, only *O. phelani* evidenced a moderate change in this character through ontogeny and, fortunately, peristome roundness is the most diagnostic trait for this species. Both remaining species exhibit little or no change during the growth of individuals. Thus, there is no danger of identifying the juvenile of one species as the adult of another.

In addition, this study indicates that there was no long-term evolutionary trend in these traits (at least in peninsular Florida) and that when the species transitions occurred, they were abrupt and show virtually no signs of gradation. For practical purposes, both of these observations lead to the conclusion that oligopygoid fossils with species-diagnostic traits intermediate to any of the three species are not to be found in numbers large enough to pose problems with the oligopygoid zonation of the Ocala Limestone in peninsular Florida.

ACKNOWLEDGEMENTS

This research was done in partial fulfillment of the requirements for the Master of Science degree, Department of Geology, University of Florida, by M. L. M. The authors would like to thank Mr. Louis Zachos of Exxon, U. S. A., P. Kier of the U. S. Museum of Natural History, and G. Shaak of the Florida State Museum for helpful discussions. For reviews of the manuscript, we also thank D. Schindel, Yale University and D. Webb, Florida State Museum.

REFERENCES CITED

American Commission on Stratigraphic Nomenclature, 1961, Code of stratigraphic nomenclature: Am. Assoc. Petroleum Geologists Bull., v. 45, p. 645.

Cheetham, A. H., 1963, Late Eocene zoogeography of the Eastern Gulf Coast Region: Geol. Soc. America Mem., v. 91, 1-113.

Chen, C. S., 1965, The regional lithostratigraphic analysis of Paleocene and Eocene rocks of Florida: Florida Geol. Survey Bull., v, 45, 1-105.

Cooke, C. W., 1915, The age of the Ocala Limestone: U. S. Geol. Survey Prof. Paper, v. 95, p. 105-176.

Croft, M., 1980, Ecology and stratigraphy of the echinoids of the Ocala Limestone [unpub. Masters thesis]: Florida State Univ., 128 p.

Kier, P., 1967, Revision of the oligopygoid echinoids: Smithsonian Misc. Coll., v. 152, p. 1-147.

McCullough, L. N., 1969, The *Amusium ocalanum* biozone [unpub. Masters thesis]: Univ. Florida, 53 p.

McKinney, M. L., 1982, Ontogeny, phylogeny, and post-depositional alteration of the oligopygoid echinoids of the Ocala Limestone [unpub. Masters thesis]: Univ. Florida, 128 p.

McKinney, M. L., and Jones, D. S., 1982, Ontogeny and phylogeny of Eocene oligopygoids from the Ocala Limestone of Peninsular Florida (Abs.): Florida Scientist Abstr. Prog., v. 45, p. 45.

Puri, H. S., 1957, Stratigraphy and zonation of the Ocala Group: Florida Geol. Survey Bull., v. 38, p. 1-248.

Puri, H. S., and Vernon, R. O., 1964, Summary of the geology of Florida and a guidebook to the classic exposures: Florida Geol. Survey Spec. Pub., v. 5, 312 p.

SAS, 1980, SAS User's Guide: Gary, N. C., SAS Institute, Inc.

Zachos, L. G., and Shaak, G. D., 1978, Stratigraphic significance of the Tertiary echinoid *Eupatagus ingens* Zachos: Jour. Paleontology, v. 52, p. 921-927.

MARINE FOSSILS FROM REGION OF TRAIL RIDGE, A GEORGIA-FLORIDA LANDFORM

By

Fredric L. Pirkle[1]
The Franklin Company
Philadelphia, Pennsylvania 19103

And

Louis J. Czel
E. I. du Pont de Nemours and Company, Inc.
Wilmington, Delaware 19898

ABSTRACT

Trail Ridge is a 130-mile-long sand ridge in northern Florida and southern Georgia. The age of this ridge and its relationship to sea-level stands have been debated by various workers for many years. Ages assigned to the ridge range from Miocene to Pleistocene. Fossils recently found along the western side of Trail Ridge, when considered in the light of other evidence, indicate that Trail Ridge is no older than late Pliocene or Pleistocene. The fossils prove that in this region, Pliocene or Pleistocene seas covered an area that now is over 130 feet above sea level.

INTRODUCTION

Trail Ridge is a 130-mile-long sand ridge that spans northern Florida and southern Georgia (Fig. 1). The age of this ridge has long been debated. Some workers believe the ridge is Miocene in age and is in fact a continuation of the Lake Wales Ridge (Alt, 1974) while other workers, for example Brooks (1966) and Pirkle and Yoho (1970), believe the ridge can be no older than Pliocene. Cooke (1939), Gillson (1959), and Grogan and others (1964) consider Trail Ridge to be a Pleistocene landform. Most attempts to date the ridge have been based on physiographic evidence, the majority of which has been drawn from studies of topographic maps and aerial photographs.

During the late summer and early fall of 1977 a series of holes was drilled along the western side of Trail Ridge in southern Georgia (Fig. 2). A jet type drilling technique described by Quirk and Eilertsen (1963) was used. Marine fossil shells, from five of the holes, were subsequently identified by Donald R. Moore of the University of Miami (Florida) School of Marine and Atmospheric Science. In addition to identifying the fossils, Moore was able to provide information concerning their probable environment of habitation. These recent findings may well alter the presently held interpretation of the geological history of Trail Ridge and certainly will have an effect on the interpretation of the history of sea level in Florida.

FOSSIL TYPES

The fossils found are gastropods, bivalve molluscs, sand dollar plates (Echinoidea), barnacle fragments, calcareous worm tubes, and two species of bryozoans. All of the fossils that could be identified are represented today by species living in shallow marine environments along the southeastern coast of the United States (Moore, written communiciation, 1977). Table 1 lists the fossils that were identified and Table 2 is a break-down by sample interval of fossils obtained from one of the drill holes. Table 2 also indicates the physical condition of the shells as they were found.

Concerning the environment of deposition Moore concludes (written communication, 1977): "The fossils indicate deposition in shallow water on a bar, or perhaps a protected area close to an inlet. Water temperatures were apparently similar to those found in northern Florida today . . . Almost all of the fossils could have lived

[1]Present address: Conoco Inc., P.O. Box 4800, The Woodlands, TX 77380.

in a lagoon, behind or on a shallow bar, or in protected water near an inlet." Moore further concludes, "The fact that these are all living species suggests a Pleistocene age for this material. The absence of extinct species also suggests a Pleistocene age." Table 3 lists the environments for some of the fossil species found.

HOST SEDIMENTS

The collar elevation of the five holes containing the fossils along the western side of Trail Ridge ranges from 158 to 170 feet above sea level (Table 4 and Fig. 2). In these holes the interval containing fossil shells ranges from 130 to 161 feet above sea level (Table 4).

Size analyses (Tables 4 and 5) were run on the intervals sampled. Typical Trail Ridge sands contain 50 to 70 percent by weight of medium sand (+ 60 mesh to - 35 mesh) and 20 to 40 percent by weight of fine sand (+ 120 mesh to - 60 mesh). These characteristics of Trail Ridge sands have been discussed by E. C. Pirkle and others (1974). In contrast to Trail Ridge sands, the sands underlying the Duval Upland east of Trail Ridge (Fig. 1) contain more than 90 percent of fine and very fine sand (+ 230 mesh to - 60 mesh). Detailed characteristics of the sands of the Duval Upland have been given by E. C. Pirkle and others (1977). Sands underlying the Northern Highlands west of Trail Ridge (Fig. 1) are more variable in grain size distribution than are sands of Trail Ridge or sands of the Duval Upland. The sediments of the Northern Highlands,

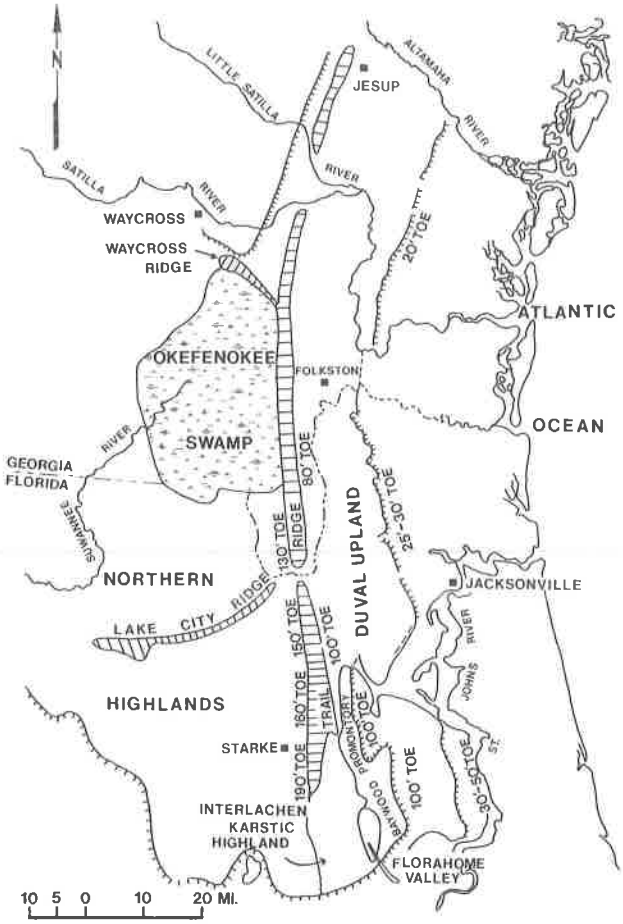

Figure 1. Location map showing Trail Ridge and other major physiographic features. Modified from E. C. Pirkle and others, 1974.

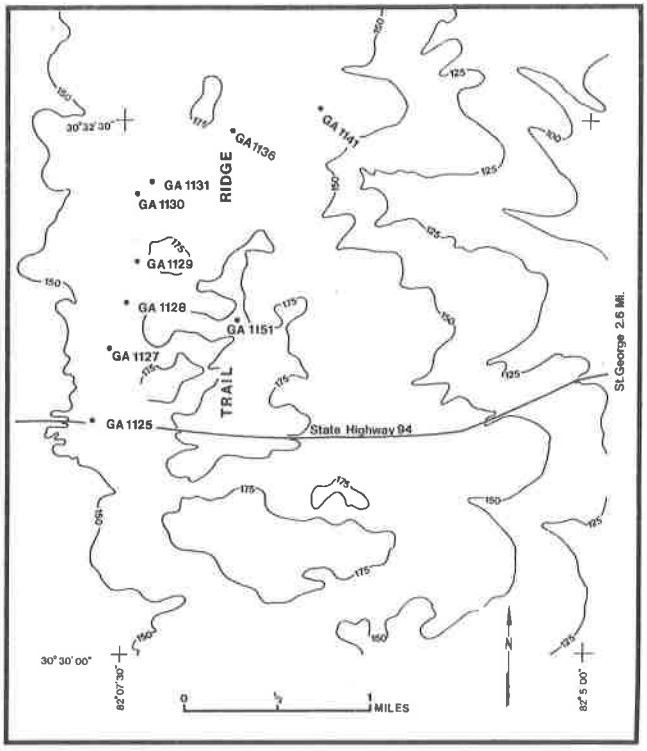

Figure 2. Drill-hole locations.

however, contain a sufficient quantity of medium-size sand grains to have served as the source materials for much of Trail Ridge. W. A. Pirkle (1972) has described the sands of the Northern Highlands.

A study of Table 4 indicates that much of the sand in the sediments penetrated by the five holes containing fossils has typical Trail Ridge sand-size distribution. It should be noted, however, that the sands, especially in the upper parts of the sequence, tend to be somewhat finer than typical Trail Ridge sands.

ORIGIN OF FOSSILIFEROUS SANDS

Since the fossiliferous materials could have several possible origins, the relationship and significance of the fossils to Trail Ridge sediments is not certain. For example, the fossiliferous sands may be a part of the high terrace sands of the Northern Highlands west of Trail Ridge. These high terrace sands are thought to be the source sediments for much of Trail Ridge and thus of an older age than the ridge (White, 1970; W. A. Pirkle, 1972; F. L. Pirkle, 1975). If this origin for Trail Ridge is correct, and the fossiliferous materials are part of the sand blanket of the Northern Highlands, then the fossils would establish the oldest age that could be assigned to Trail Ridge.

It is possible, however, that the fossiliferous sediments were deposited in inlets or in a small embayment that formed when Trail Ridge was breached in post-Trail Ridge time by seas encroaching from the east. A breach in Trail Ridge sediments might be traced by using finer-grained sand, or at least a grain-size distribution different from that of Trail Ridge sand, as a guide. Sand size data from Tables 4 and 5 suggest that such a breach might have occurred. Finer-grained materials do overlie coarser, more typical Trail Ridge sands in some of the holes.

An examination of heavy minerals might shed light on the problem, especially if the source sediments of the fossiliferous sands were different from the source sediments of Trail Ridge sands. The Trail Ridge heavy-mineral suite has been described by Cannon (1950), Pirkle and Yoho (1970), and Garnar (1972). It contains no garnet,

Table 1. List of fossil species.

	Mollusca - Bivalvia	No.
1.	*Mulinia lateralis* (Say, 1822)	28
2.	*Nucula proxima* (Say, 1822)	8
3.	*Gemma gemma* (Totten, 1834)	9
4.	*Cumingia tellinoides* (Conrad, 1841)	1
5.	*Chione cancellata* (Linne, 1767)	1
	Gastropoda	
6.	*Nassarius trivittatus* (Say, 1822)	2
7.	*Mitrella lunata* (Say, 1826)	2
8.	*Turbonilla sp.*	1
9.	*Retusa canaliculata* (Say, 1822)	4
10.	*Kurtziella cerina* (Kurtz & Stimpson, 1851)	1
11.	*Natica pusilla* (Say, 1822)	2
12.	*Olivella sp.*	1
13.	*Triphora nigrocincta* (C. B. Adams, 1839)	1
14.	*Mellita quinquiesperforata* (Leske, 1778) (Echinoid)	6 fragments
	Bryozoa	
15.	*Schizoporella unicornis* ???? (Johnston, 1847)	abundant
16.	*Discoporella doma* ???? (d'Orbigny, 1852)	few pieces
	Annelida - Palychaeta	
17.	*Hydroides norvegica* ???? (Gunner, 1768)	fragments

Table 2. List of species from the samples of hole GA1125.

	0-5 feet	No.
1.	*Mulinia lateralis*	4 va.
2.	*Gemma gemma*	1 va.
3.	*Turbonilla sp.*	1 pi.
4.	*Olivella sp.*	1 pi.
5.	*Schizoporella*	18 pi.
6.	*Discoporella*	2 pi.

	10-15 feet	
1.	*Mulinia lateralis*	12 pi.
2.	*Gemma gemma*	2 pi.
3.	*Chione cancellata*	1 pi.
4.	*Nucula proxima*	1 va. & 1 frag.
5.	*Indeterminate bivalve frags.*	11
6.	*Retusa canaliculata*	1
7.	*Kurtziella cerina*	1
8.	*Mitrella lunata*	1
9.	*Nassarius trivittatus*	1 + 1 frag.
10.	*barnacle*	Sev. frags.
11.	*Hydroides*	6 pi.
12.	*Mellita quinquiesperforata*	4 frags.
13.	*Schizoporella*	30 frags.
14.	*Discoporella*	7 frags.

	15-20 feet	No.
1.	*Nucula proxima*	5 pi.
2.	*Gemma gemma*	3 va. + 2 frags.
3.	*Mulinia lateralis*	1 + 11 frags.
4.	*Retusa canaliculata*	2 + 1 frag.
5.	*Triphora nigrocineta*	1
6.	*Natica pusilla??*	1
7.	*Mitrella lunata*	1
8.	*Indeterminate gastropods*	2 frags.
9.	*Hydroides*	10 frags.
10.	*Mellita quinquiesperforata*	2 frags.
11.	*Schizoporella*	22 frags.
12.	*Discoporell*	12 frags.
13.	*Barnacle*	2 frags.

	20 - 25 feet	
1.	*Mulinia lateralis*	2 pi.
2.	*Gemma gemma*	1 pi.
3.	*Cumingia tellinoides*	1 pi.
4.	*Nucula proxima*	1 va.
5.	*Natica pusilla?*	1
6.	*Mellita quinquiesperforata*	2 pi.
7.	*Schizoporella*	9 pi.
8.	*Discoporella*	3 pi.
9.	*barnacle*	1

	25 - 26 feet	
1.	*Nucula proxima*	1 pi.
2.	*Schizoporella*	2 pi.

Note: va. = valve
pi. = piece
frag. = fragment

Table 3. Habitat of some of the fossils encountered.

Fossil Species[1]	Environmental Conditions[1]
Mulinin lateralis	Lives in shallow bays or lagoons. Rarely found offshore. Can withstand both reduced and increased salinities, usually lives in lower salinity waters.
Nucula proxima	Often found living offshore but also found living in shallow lagoons along with *Gemma gemma, Chione cancellata, Mulinia lateralis,* and *Cumingia tellinoides.*
Gemma gemma	Lives in more marine parts of shallow bays and lagoons. Rarely found living offshore.
Cumingia tellinoides	Lives in shallow bays and lagoons.
Chione cancellata	Lives in more marine parts of shallow bays and lagoons. Rarely found living offshore.
Nassarius trivittatus	Prefers protected waters of shallow lagoons. Sometimes lives a little offshore.
Mitrella lunata	Prefers protected waters of shallow lagoons. Sometimes lives a little offshore.
Retusa canaliculata	Lives in shallow marine sandy habitats both inshore and offshore.
Mellita quinquiesperforata	Lives just off the beach in shallow water about 4 to 30 feet deep. It is not found in lagoons.
Schizoporella	Lives in shallow water both open sea and lagoons.
Discoporella	Prefers sandy muddy bottoms offshore.

[1]From Donald R. Moore, written communication, 1977

no epidote, and no hornblende. In contrast, the Atlantic Coast suite, which is characteristic of surface sands in many areas east of Trail Ridge, contains these three minerals (Cannon, 1950). The heavy-mineral suite of the fossiliferous sands penetrated along the western side of Trail Ridge was examined and, indeed, is similar to that of the Atlantic Coast suite. Garnet, epidote, and hornblende are present in the sands of the fossiliferous sediments. The same Atlantic Coast heavy-mineral suite occurs in ridges of fine sand banked up along the eastern side of Trail Ridge in Clay County in northern peninsular Florida (Pirkle and Yoho, 1970).

Allowing that the fossiliferous sands accumulated in inlets or a shallow embayment as seas encroaching from the east breached Trail Ridge, then Trail Ridge must be older than the sands containing the fossils. Therefore the age of the fossiliferous sands would establish the youngest possible age for Trail Ridge.

There are studies in progress that may be used to establish the oldest age that can be assigned to parts of Trail Ridge. Extensive peat occurrences underlie Trail Ridge in some regions (Pirkle and Yoho, 1970), and work at the Pennsylvania State University and South Dakota School of Mines and Technology indicates that these peats are late Pliocene or more likely Pleistocene in age (Rich, F., personal communication, 1982). A confirmation of this age by continuing studies would allow a maximum age for parts of Trail Ridge to be established. In short, if the fossiliferous sands described in this report are younger than Trail Ridge, and the peats underlying Trail Ridge are

late Pliocene or Pleistocene in age, the time interval during which Trail Ridge was formed can be narrowed considerably. Trail Ridge could not be Miocene in age, it would have to be late Pliocene or Pleistocene.

SUMMARY AND CONCLUSIONS

Marine fossils were found in five holes drilled along the western side of the topographic expression of Trail Ridge in southern Georgia. These fossils are believed to be late Pliocene or Pleistocene in age and indicative of a shallow marine environment.

Studies of the fossils, comparisons of the grain-size distribution of quartz sands, and examinations of heavy-mineral suites indicate that the fossiliferous sands were probably deposited in inlets or a shallow marine embayment as seas encroaching from the east breached Trail Ridge in post-Trail Ridge time. This sequence of events results in the fossils establishing the youngest possible age for Trail Ridge.

In some areas Trail Ridge occurs over extensive deposits of peat. The peat accumulations may be late Pliocene or Pleistocene in age. Should these ages prove to be correct, the oldest possible age for these parts of Trail Ridge must be late Pliocene or Pleistocene.

Even though the fossils cannot be used for precise dating of Trail Ridge, in part because of the uncertainty of the origin of the fossiliferous sands, the fossils do furnish the strongest evidence thus far offered that late Pliocene or Pleistocene seas covered

Table 4. Analyses of samples from drill holes containing marine fossils. See Figure 2 for hole locations.

Hole I.D.	Collar Elev. (Ft. above sea level)	Fossilliferous Interval (Ft. above sea level); depth below land surface (in ft.)	Sample Interval (Ft. below land surface)	Percent of Sand Retained on Mesh 16	20	35	60	120	230	Pan
GAI125	158	132-158; 0-26	0-5	0.28	0.33	11.55	41.01	40.56	5.21	1.06
			5-10		0.37	11.98	45.24	38.32	3.34	0.75
			10-15	1.06	0.77	8.13	36.45	47.67	4.74	1.18
			15-20	1.09	0.46	10.51	42.47	41.18	3.46	0.83
			20-25	0.59	0.35	8.87	40.74	44.33	3.78	1.34
			25-26	0.21	0.12	10.83	39.36	44.81	3.11	1.78
GAI127	169	138-160; 9-31	0-5		0.15	9.81	47.73	38.08	3.62	0.61
			5-10		0.34	10.92	48.20	37.57	2.37	0.60
			10-15		0.25	9.70	46.71	37.66	3.70	1.98
			15-20		0.07	10.73	57.75	27.43	2.69	1.33
			20-25		0.22	23.62	53.11	20.90	1.72	0.43
			25-30		0.09	11.06	50.78	34.66	2.72	0.69
			30-35		0.09	6.92	48.74	41.28	3.23	0.74
			35-40		0.26	13.94	51.35	30.47	3.07	0.91
GAI128	167	147-152; 15-20	0-5		0.30	12.45	46.06	35.46	4.67	1.06
			5-10		0.26	11.38	43.21	38.02	5.31	1.82
			10-15		0.09	7.10	47.20	39.03	5.21	1.37
			15-20		0.17	11.20	46.41	37.60	3.35	1.27
			20-25		0.17	14.62	49.42	33.22	2.21	0.36
			25-30		0.26	14.62	55.10	26.32	2.91	0.79
			30-35		0.19	17.44	57.54	21.80	2.19	0.84
			35-38		0.12	13.75	56.99	26.86	1.95	0.33
			38-40		0.02	5.01	38.11	51.20	3.90	1.76
GAI129	169	152.5-161; 8-16.5	0-5		0.20	9.56	43.78	39.89	5.18	1.39
			5-10		0.24	9.45	44.57	41.95	2.93	0.86
			10-15		0.19	8.97	42.58	41.86	4.79	1.61
			15-20		0.20	7.68	41.10	44.92	3.78	2.32
GAI130	170	?-155; 15-?	0-5		0.25	10.72	44.67	38.21	4.49	1.65
			5-10		0.26	11.75	51.09	32.33	2.88	1.66
			10-15		0.21	15.18	51.51	27.16	4.59	1.28
			15-20		0.10	15.19	48.93	29.05	4.70	1.69
			20-25		0.55	17.85	50.57	24.45	4.22	1.92
			25-30		0.24	24.82	51.64	20.52	1.70	0.55

Table 5. Analyses of samples from drill holes not containing marine fossils. See Figure 2 for hole locations.

Hole I.D.	Collar Elev. (Ft. above sea level)	Sample Interval (Ft. below land surface)	Percent of Sand Retained on Mesh						
			16	20	35	60	120	230	Pan
GA1131	172	0-5		0.26	10.72	44.67	38.21	4.49	1.65
		5-10		0.29	11.75	51.09	32.33	2.88	1.66
		10-15		0.28	15.18	51.51	27.16	4.59	1.28
		15-20		0.35	15.19	48.93	29.05	4.79	1.69
		20-25		0.99	17.85	50.57	24.45	4.22	1.92
		25-30		0.77	24.82	51.64	20.52	1.70	0.55
GA1136	171	0-5		0.58	15.20	45.76	34.83	3.10	0.53
		5-10		0.83	14.09	44.21	35.29	3.33	2.25
		10-15		0.61	16.48	57.88	22.93	1.60	0.50
		15-20		0.21	13.00	58.70	25.88	1.62	0.59
		20-25		0.15	14.01	57.46	25.32	2.18	0.88
		25-30		0.13	14.69	55.41	25.80	2.98	0.99
GA1141	165	0-5		0.45	14.77	45.41	34.21	4.16	1.00
		5-10		0.38	12.36	47.84	36.12	2.43	0.87
		10-15		0.45	10.39	44.70	41.21	2.54	0.71
		15-20		0.61	14.99	46.68	33.24	3.14	1.34
		20-25		0.29	15.89	50.85	29.61	2.48	0.88
		25-30		0.08	12.27	49.22	34.98	3.02	0.43
GA1151	176	0-5		0.81	17.47	47.26	30.75	3.13	0.58
		5-10		1.67	22.54	42.58	29.72	3.28	1.32
		10-15		1.14	24.59	49.21	22.21	2.19	0.66
		15-20		1.04	20.81	54.92	20.31	2.10	0.82
		20-25		0.28	17.86	55.59	22.76	2.32	1.19
		25-28.5		0.22	16.05	58.75	23.16	1.37	0.45
		28.5-30		0.16	12.11	55.21	28.77	2.55	1.20

areas in southern Georgia and northern Florida that now are between 130 and 160 feet above sea level. Assuming the sands are Pleistocene in age as indicated by the fossils, and Pleistocene sea level rose no more than 5 meters above present sea level due to melting of glacial ice, then the present elevation of these fossiliferous sands must be due in large part to uplift, either from tectonic forces or as a response to isostatic adjustment.

REFERENCES CITED

Alt, D., 1974, Arid climatic control of Miocene sedimentation and origin of modern drainage, southeastern United States, *in* Post-Miocene stratigraphy, central and southern Atlantic Coastal Plain, Oaks, R. Q., Jr., and DuBar, J. R., eds.: Utah State University Press, p. 21-29.

Brooks, H. K., 1966, Geological history of the Suwannee River, *in* Olsen, N. K., ed., Geology of the Miocene and Pliocene series in the North Florida-South Georgia area: Atlantic Coastal Plain Geological Association 7th Field Trip, Southeastern Geological Society 12th Field Trip, Guidebook, p. 37-45.

Cannon, H. B., 1950, Economic minerals in the beach sands of the southeastern United States: Symposium on Mineral Resources of the Southeastern United States, University of Tennessee Press, p. 202-210.

Cooke, C. Wythe, 1939, Scenery of Florida interpreted by a geologist: Florida Geological Survey Bull. 17.

Garnar, T. E., Jr., 1972, Economic Geology of Florida heavy mineral deposits, *in* Puri, H. S., ed., Proc. 7th Forum Geology of Industrial Minerals: Florida Bureau of Geology Spec. Pub. 17, p. 17-21.

Gillson, J. L., 1959, Sand deposits of titanium minerals: Min. Eng., v. 11, p. 421-429.

Grogan, R. M., Few, W. G., Garnar, T. E., and Hager, C. R., 1964, Milling at Du Pont's heavy mineral mines in Florida, *in* Arbiter, N., ed., Milling Methods in the Americas: VII International Mineral Processing Congress, New York, Gordon and Breach Science Publishers, p. 205-229.

Pirkle, E. C., Pirkle, W. A., and Yoho, W. H., 1974, The Green Cove Springs and Boulougne heavy-mineral sand deposits of Florida: Economic Geology, v. 69, p. 1129-1137.

Pirkle, E. C., Pirkle, W. A., and Yoho, W. H., 1977, The Highland heavy-mineral sand deposit on Trail Ridge in northern peninsular Florida: Florida Bureau of Geology Report of Investigation No. 84, 50 p.

Pirkle, E. C., and Yoho, W. H., 1970, The heavy mineral ore body of Trail Ridge Florida: Economic Geology, v. 65, p. 17-30.

Pirkle, F. L., 1975, Evaluation of possible source regions of Trail Ridge sands: Southeastern Geology, v. 17, p. 93-114.

Pirkle, W. A., 1972, Trail Ridge, relic shoreline feature of Florida and Georgia [Ph.D. dissert.]: Chapel Hill, Univ. North Carolina, 86 p.

Quirk, R. and Eilertsen, N. A., 1963, Methods and costs of exploration and pilot plant testing of ilmenite-bearing sands, Lakehurst Mine, The Glidden Co., Ocean County, N. J.: Bureau of Mines Information Circular 8197.

White, W. A., 1970, The geomorphology of the Florida peninsula: Florida Bureau of Geology Bull. 51, 164 p.

THE MONTEAGLE LIMESTONE (MISSISSIPPIAN) IN NORTH CENTRAL TENNESSEE: PETROLOGY, POROSITY, AND SUBSURFACE GEOLOGY

By

David N. Lumsden, C. Darrel Norman, and Barry J. Reid
Department of Geology
Memphis State University
Memphis, Tennessee 38152

ABSTRACT

The Monteagle Limestone was studied using subsurface methods in Morgan, Scott, and Fentress counties and at outcrops in adjacent Putman, Overton and Campbell counties in Tennessee. Eight to ten repetitions of a simple shallowing upward lithologic cycle are present in the outcrop sequences. The cycle starts with a fossiliferous packstone-grainstone, passes upward into an oolitic grainstone, and is capped by either a lime mudstone (or dolomudstone), a peloidal packstone-grainstone or a wackestone. Minor shales and intraclast packstone-grainstones are also present. Primary porosity may be preserved in the uncompacted oolitic grainstones but has been destroyed by compaction and void filling calcite in the fossiliferous packstone-grainstones. Isopact maxima in net porosity trend NNE-SSW, and are superimposed on *thin* net thickness trends.

INTRODUCTION

The Monteagle Limestone is a gas productive unit in north central Tennessee. Little has been published on Monteagle petrology or facies pattern in the area and our goal here is to supply such information, both as an aid in advancing our understanding of Mississippian historical geology and as an aid in defining potential productive hydrocarbon trends.

The Monteagle Limestone (Vail, 1957; Stearns, 1963) is a Middle Mississippian carbonate dominated by an oolitic grainstone lithology (Fig. 1). It is partially correlative with the St. Genevieve Limestone of the Illinois Basin area (Milici and others, 1979). To the south the Monteagle maintains its lithologic character across the Cumberland Plateau (Handford, 1978) finally grading into clastic sediments in Alabama and Georgia (Thomas, 1972). To the east it grades into the Newman Limestone (Milici and others, 1979), and the west, towards the Central Basin of Tennessee, it has been removed by erosion.

The study area is in the Cumberland Plateau region (Fig. 2), an area that, during Mississippian, was a portion of the Appalachian shelf, a tectonically stable feature where a thick, uniform veneer of largely carbonate rocks was deposited.

METHODS

Density logs from 79 wells, selected to form a uniform distribution over the area of Scott, Morgan, and Fentress counties, were used to prepare a structure contour map, net thickness map, net thickness with more than 4 percent porosity isopach map, and a net thickness with more than 10 percent porosity isopach map. Porosity was estimated from the formation density logs. Computer drawn maps gave the same patterns as hand contoured maps and served to confirm our interpretation. Relevant data are tabulated in Reid (1981). A type log in Figure 3 illustrates the "kicks" used for top and bottom criteria on the logs. The contact with the overlying Big Clifty (Hartselle) Sandstone is fairly easy to pick; however, the Big Clifty is not everywhere present. The contact with the underlying St. Louis Limestone is much more difficult to select. The St. Louis is dolomitic, cherty, and more dense than the Monteagle. The transition between the two units can be followed by correlating "kicks" in density logs. Sample logs obtained from the Tennessee Division of Geology files were used to supplement the density log interpretations.

SYSTEM	FORMATION	THICK.	LITHOLOGY
MISSISSIPPIAN	PENNINGTON FM.	150 To 450 Ft.	SHALE AND SILTSTONE (RED AND GREEN), SANDSTONE, DOLOSTONE AND LIMESTONE.
	BANGOR LS.	150 To 300 Ft.	LIMESTONE, FOSSILIFEROUS, OOLITIC IN PART.
	BIG CLIFTY FM.	0 To 60 Ft.	SANDSTONE, SANDY LIMESTONE, FOSSILIFEROUS SHALE, DOMINANT LITHOLOGY IS VARIABLE.
	MONTEAGLE LS.	150 To 275 Ft.	LIMESTONE, FOSSILIFEROUS, OOLITIC & CROSS-BEDDED IN PART.
	ST. LOUIS LS.	MAX. 110 Ft.	LIMESTONE & DOLOSTONE, CHARACTERIZED BY LITHOSTROTION CORAL.
	WARSAW LS.	MAX. 80 Ft.	LIMESTONE, ARENACEOUS, CROSS-BEDDED IN PART.
	FT. PAYNE FM.	MAX. 190Ft.	LIMESTONE AND DOLOSTONE, VERY SILICEOUS.
DEVONIAN	CHATTANOOGA SH.	0 To 40 Ft	SHALE, DARK GRAY TO BLACK, BITUMINOUS, FISSILE.

Figure 1. The generalized Mississippian stratigraphic terminology of the study area. Modified from Stearns (1963). The term Big Clifty *was reintroduced by Roberts and Lumsden (1982) in place of the term* Hartselle.

Figure 2. Location maps. Outcrop locations are labeled L1 (Livingston-1), L2 (Livingston-2), C (Cookeville-2), and J (Jellico). Peterson's section 78/79 is labeled P (Peterson, 1962). The subsurface map area is outlined heavily. Data for the subsurface study are given in Reid (1981). The L1, L2, and C outcrop data are in Norman (1981). The data for the Jellico outcrop are in Gregory (1981). The small irregular outlines in Scott, Morgan, and Fentress Counties represent gas fields in the Monteagle.

As there were no cores available, lithologic data were obtained from samples collected at 3 locations to the west of the subsurface area and one location east of the subsurface area (Fig. 2). Standard thin sections were prepared and stained to facilitate calcite/dolomite identification (Lindholm and Finkleman, 1972). Thin sections were point counted to determine component proportions. X-ray diffraction was used to determine dolomite nonstoichiometry following the method of Lumsden and Chimahusky (1980). Relevant analytical data are tabulated in Norman (1981) or Gregory (1981).

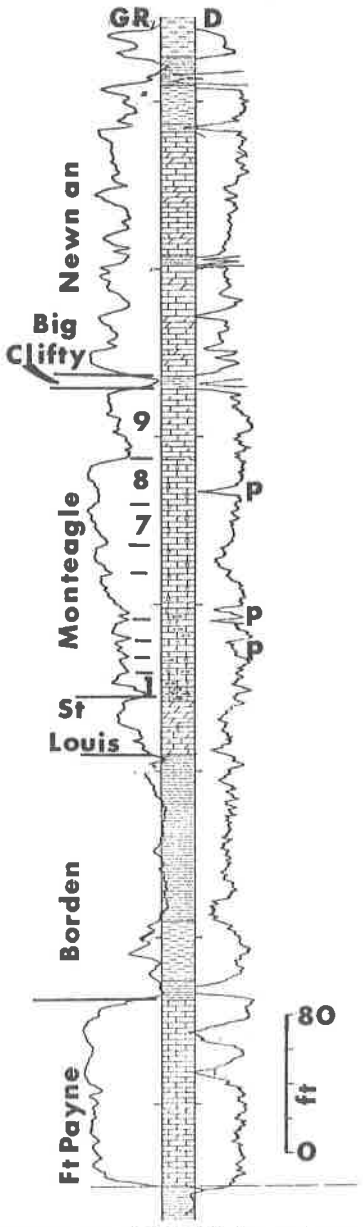

Figure 3. A portion of the gamma ray (GR)-density (D) log of the Collins No. 3 Whaley well in Oneida West Field, Scott County, Tennessee. The "p" to the right of the column marks porous zones in the Monteagle. The interpretation of nine cycles in the gamma ray trace of the Monteagle is suggested by our interpretation of outcrop variations. (See Figure 8.) Note the relatively distinct Monteagle-Big Clifty (Hartselle) pick and the interpretative nature of the Monteagle-St. Louis pick. Modified from Webb (1972).

RESULTS

Subsurface

Structure Map: Figure 4 illustrates the structure on the top of the Monteagle. Notable is the rather simple parallelism of the contours and the N 25 to 30° E strike. There is a gradual eastward increase in dip from approximately 0.5° in the west to 1.5° to

the east. These results are in essential agreement with a similar map in Keplinger (1980); however, Keplinger found dips of less than 0.5 degrees in the east area.

Isopachous Maps: Monteagle thickness varies from 210 to 270 feet over the subsurface study area (Fig. 5). The pattern of thickness variation suggests a Monteagle-thin trend bearing N 70°E crossed in the middle of the map by another Monteagle-thin trend bearing N 20°E. There appears to be more variation in thickness within the map area than there is from one edge to another suggesting that the depositional environment was of essentially uniform water depth. Thinning and thickening within the map area may reflect local concentration of sediment by current and wave action or buildups initiated on pre-Monteagle topographic high points.

Both the isopachous maps of the aggregate thickness with more than 4 percent porosity (Fig. 6) and more than 10 percent porosity (Fig. 7) show a thick porosity zone trending approximately N 25° to 35°E. These trends overlie and parallel the *thin* trend in the net thickness isopach map (Fig. 5).

Lithofacies

Seven lithofacies are present, 6 carbonate, named according to Dunham's classification (1962), and shale. The proportion of various lithologic components at the four outcrop locations and the proportion of the various lithofacies described below are illustrated in Figure 8.

Oolitic grainstones dominate the Monteagle. The oolite nuclei composition reflects the composition of underlying units, either skeletal debris or micrite clasts. The oolites have a thick cortex. Although dolomite is uncommon, individual samples may have up to 60 percent dolomite with some development of shrinkage porosity. Beds are thick with both one and two directional cross beds. The fabric is open and uncompacted with calcite spar commonly filling the intersticies between grains (Fig. 9).

There is a greater proportion of non-oolite grains, both skeletal and peloid, in the oolitic grainstones at Jellico than at the three western outcrops (Fig. 8).

A comparison of the lithology with modern analogs (e.g. Newell and others, 1960;

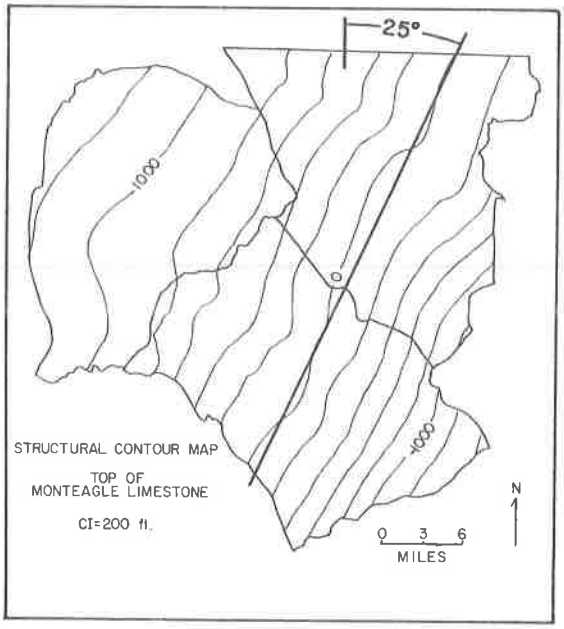

Figure 4. A structure contour map on the top of the Monteagle Limestone. A distinct N25°E strike is apparent.

Ball, 1967) suggests a very shallow water (2.0 m), open marine environment of deposition where strong currents and waves could remove fine sediment and keep the oolite grains suspended at least part of the time. The uncompacted texture suggests early cementation.

Fossiliferous packstone-grainstones are the second most abundant lithology. Composition varies widely from "pure" packstone to "pure" grainstones. The group is united by the high proportion of skeletal debris (55 percent), mostly echinoderm and bryozoan fragments. Dolomite is not abundant (0-21 percent). Echinoderm-dominated samples are grainstones; bryozoan-dominated samples tend to have more micrite (packstones), a trait also noted by Handford (1978). Many skeletal fragments in the fossiliferous grainstones have a micrite coating with a smooth outer surface and an irregular inner margin. Although some of these coatings may be oolitic, the majority are probably the result of replacement resulting from the precipitation of calcium carbonate in discarded algal bores (Bathurst, 1976). Overall, fossiliferous packstone-grainstones have a crowded, compacted, fabric with abundant sutured grain contacts (Fig. 10); a texture that contrasts sharply with that of the oolite grainstones (Fig. 9). One direction cross-beds dipping north are common, particularly at the Livingston 2 exposure. Units of this lithology commonly underlie oolitic grainstone units.

This lithology represents a spectrum of energy conditions associated with shallow subtidal marine waters.

Peloidal packstone-grainstones. Peloids in the form of fecal pellets, small intraclasts, and micritized fossils average 40 percent, skeletal debris forms 18 percent, lime mud 22 percent, calcite spar 17 percent, and other components form 3 percent of the average sample of this lithology. Dolomite ranges from 11 to 40 percent mostly as rhombs replacing lime mud. This lithology commonly overlies oolite grainstones.

Comparison with modern analogs (Bathurst, 1976) suggest that this lithology was deposited in an intertidal environment less subject to drying than the lime mudstone-dolomudstone situation.

Fossiliferous and peloidal packstone/grainstones are somewhat less common at Jellico compared to the western outcrops (Fig. 8).

Lime mudstones (and dolomudstone) form 10 percent of the Monteagle. Fenestral spar is common. Dolomite ranges from 0 to 100 percent, and peloids are ubiquitous.

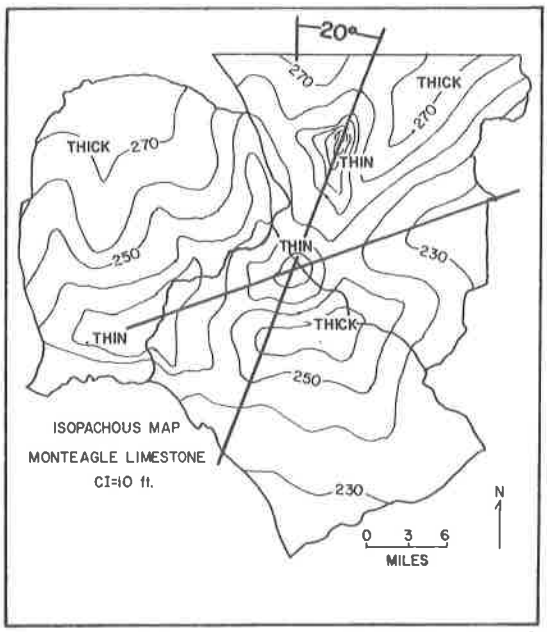

Figure 5. An isopachous map of the Monteagle Limestone. Trends of thins are marked by solid lines.

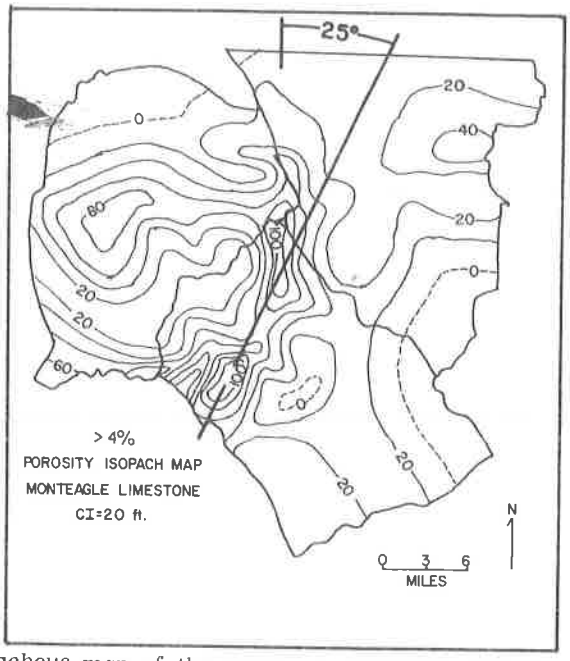

Figure 6. An isopachous map of the aggregate thickness with greater than 4 percent porosity in the Monteagle Limestone. A significant thick trend, marked by the solid line, nearly coincides with the thin trend in aggregate thickness in Figure 5.

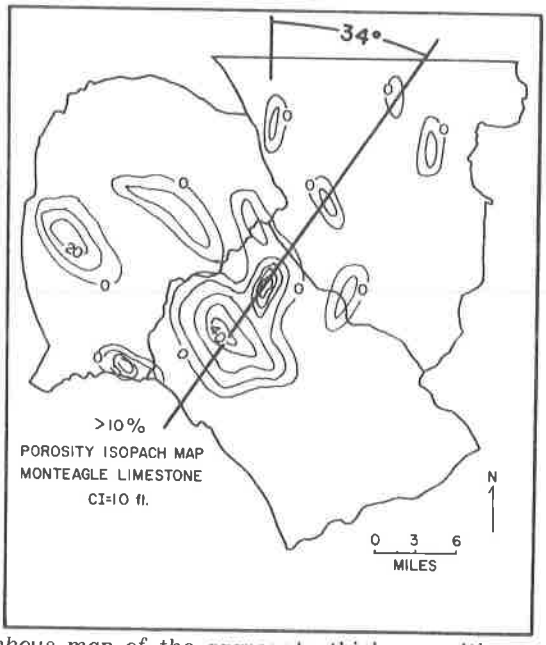

Figure 7. An isopachous map of the aggregate thickness with greater than 10 percent porosity in the Monteagle Limestone. A suspected thick trend is marked by the solid line. This trend approximates a similar trend in Figure 6.

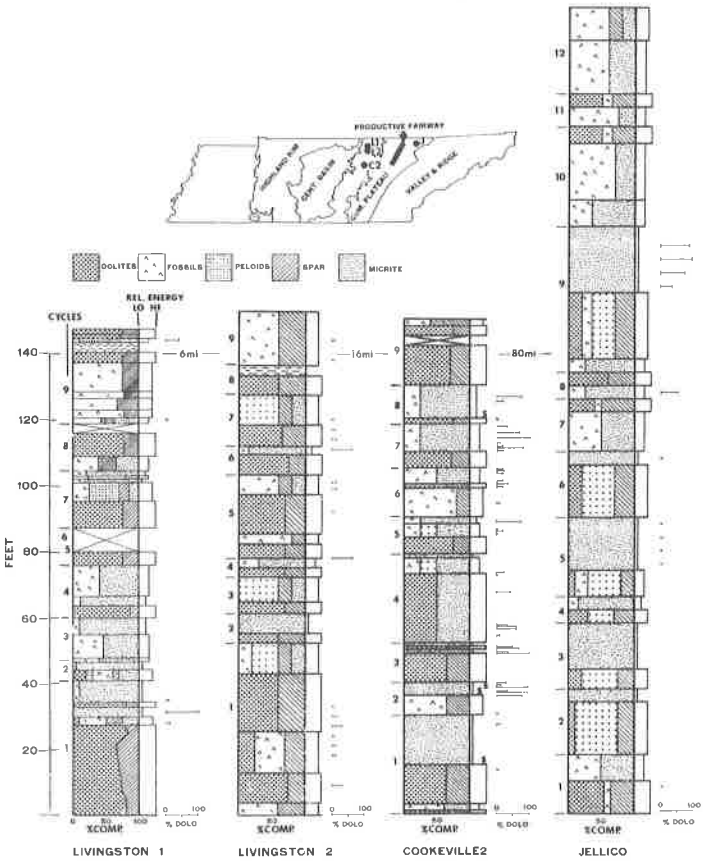

Figure 8. Columnar sections showing the relative variation in the five major lithologic components (oolites, fossils, peloids, spar and micrite) at each of the four study locations. The profiles on the right of each column show the variation in relative environmental energy for various subintervals (highest energy assigned to oolitic grainstones, lowest to micrites). Bars to the right of the energy profile show the proportion of dolomite in samples. Cycles numbered to the left of the column represent subjective interpretations of vertical repetitions in lithology. Alternative patterns can be selected but 9 to 10 cycles are present in the western 3 outcrops in most interpretations. Note the relative decrease in oolites and increase in micrite at Jellico relative to the western 3 outcrops. Similar cycles can be seen in Peterson's (1962) columnar sections. Shale breaks are marked by S letters along the right edge of the Cookeville 2 section. A presistent shale bed is found at the top of the Monteagle at the 3 western locations.

Lime mudstone units usually overlie oolitic grainstones. Analogy to sediments with fenestral structures in modern tidal flats (Shinn, 1964, 1968; and Shinn and others, 1969) suggests that these lithologies were deposited in supratidal and intertidal environments.

Wackestones form 6 percent of the measured sections. Dolomite content ranges from 0 to 64 percent, largely as rhombs replacing calcite micrite. Ostracode fragments dominate the grains. Although the ostracodes usually are randomly oriented, they may occur in fossil-rich laminations wherein they are subparallel to one another.

Wackestones are polygenetic and do not occur in any obvious systematic stratigraphic position. Where they are dolomitic with abundant fenestral patches of spar they probably were deposited in supratidal environments. More uniform nondolomitic units are subtidal deposits (Shinn, and others, 1968).

Wackestones and carbonate mudstones are notably more common at Jellico than at the western outcrops (Fig. 8).

Intraclast packstone-grainstones form less than 1 percent of the measured section. The few units of this lithology may have formed as storm deposits; however their association with lime or dolomite mudstones suggests channel deposits on tidal flats (Shinn and others, 1969).

Shales form 2 percent of the Monteagle. They occur both as thin layers associated with lime mudstone, wackestone, and peloidal packstone-grainstone units and in the LaFollet Member, a regionally widespread shale unit several feet thick that occurs near the top of the Monteagle.

Lineation

The NNE to SSW trend in porosity that we observe in the Monteagle is similar to the orientation of Monteagle oolite shoals as suggested both by Vail (1959) and Handford (1978). In Indiana, Carr (1973) noted that the porous interior of Ste. Genevieve oolite bodies parallel the gross thickness trend of the oolite body. Similarly we believe that our porosity trends mimic and parallel oolite shoal thickness trends. Choquette and Steinen (1980) document a similar NNE-SSW orientation in oolite bars of the age equivalent Ste. Genevieve of the southern Illinois Basin. They infer a paleoshoal area with the orientation of oolite bars controlled by tidal currents that ebbed and flowed approximately perpendicular to the trend of the shoal. Such a relationship was reported in modern oolite shoals by Ball (1967). In the Monteagle porosity trends are coincident with thin trends in the net thickness isopach of the Monteagle. This suggests that the oolite shoals were localized on pre-Monteagle topographic high points.

The Monteagle apparently thins sharply just west of the subsurface area. Thicknesses at the measured sections average close to 150 feet whereas thicknesses in the subsurface and at Jellico are 250 feet or more. This further supports the presence of a paleoshoal area similar to that documented in Choquette and Steinen (1980). The greater abundance of micrite-dominated lithologies at Jellico vis-a-vis those in the western outcrops may be a reponse to inner shelf conditions similar to those of the interior of the modern Bahama Bank (Ball, 1967).

Lateral Variation

The 3 western outcrops are markedly similar to each other (Fig. 8). In fact, with a little interpretation it is possible to correlate individual lithologic cycles from

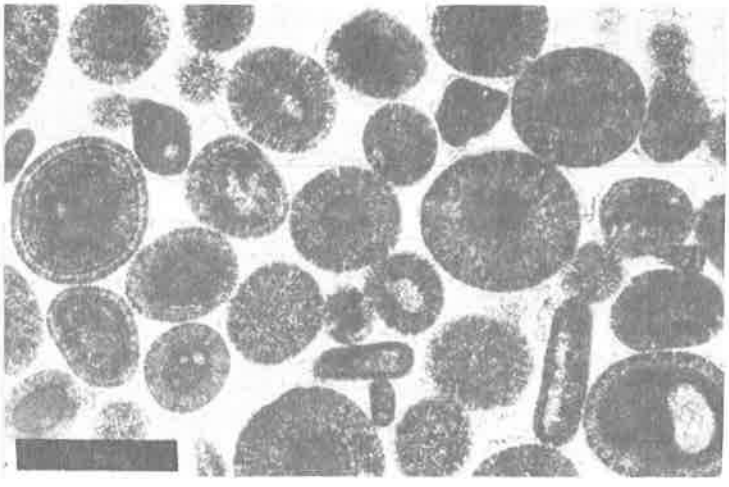

Figure 9. A photomicrograph of an oolitic grainstone. Note the open uncompacted texture and thick grain cortex. Alizarin stained, uncrossed nicols, 0.5-mm bar, sample from the Cookeville 1 location.

Livingston 1 to Cookeville 2. The same sequence of lithologic variation is also present in outcrops studied by Peterson (1962) suggesting that this depositional sequence can be correlated 65 km (40 mi) north-south. In contrast, comparison of the western outcrops with the Jellico section suggests as many differences as similarities. In particular micrite is more abundant with fewer oolite and more peloid grains at Jellico (Fig. 8). This suggests conditions remarkably similar to the situation studied by Choquette and Steinen (1980) in the distant Illinois Basin; that is to say, a north-south trending, oolite grainstone dominated, paleoshoal with vertically and laterally associated micrite dominated deposits.

DISCUSSION

Depositional Cycles

Simple counts of the number of transitions of one lithology to another coupled with considerations of thicknesses and the lateral persistence of beds in outcrop suggest that there are eight to ten repetitions of the lithologic sequence, illustrated in Figure 11, in the outcrops studied (Fig. 8). The cycle begins with a fossiliferous packstone-grainstone. This is gradationally overlain by an oolitic grainstone which, in turn, is overlain by one of several micrite dominated lithologies. This cycle is similar to one suggested by Choquette and Steinen (1980) for the Ste. Genevieve Limestone of the Illinois Basin. They start their cycle with the dolomitic lime mudstone-wackestone, a lithology that commonly caps our cycle.

The packstone-grainstones that begin the cycle are dominated by uncoated or thinly coated grains, have varying amounts of lime mud and occasional one directional crossbeds. They may contain peloids of intraclast origin and bryozoa with mud filled zooecia derived from underlying mudstone units. The fossils are normal marine robust forms typical of middle Paleozoic limestones. This rock type undoubtedly is a consequence of a shallow subtidal, open marine shelf environment (Handford, 1978). Water depths probably ranged from 2 to 30 meters in depth.

As water depths shallowed, production of ooids reached an optimum and broad expanses of oolitic tidal bars developed over the shelf. The tidal bars migrated under the influence of tidal currents, resulting in a NNE-SSW orientation for most bars (Vail, 1959; Handford, 1978; Figs. 6 and 7). The upward transition from one-directional to two-directional crossbeds indicates deposition influenced by either flood or ebb tides followed by deposition influenced by both flood and ebb tides, a feature indicative of

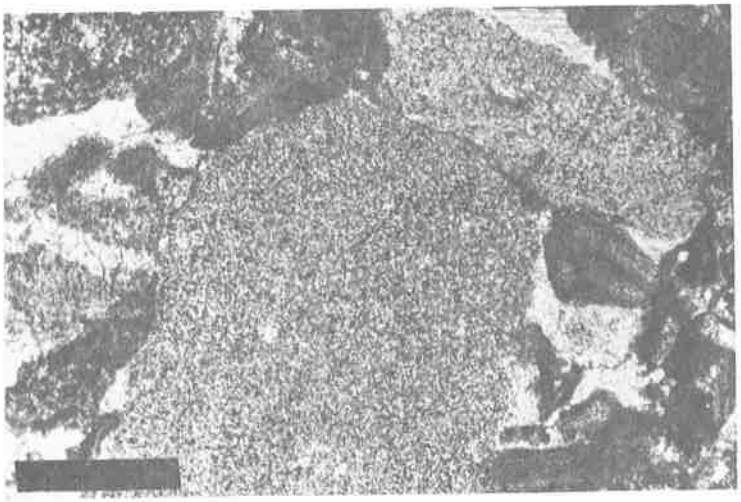

Figure 10. A photomicrograph of a fossiliferous packstone illustrating the compacted texture, microstylolitic grain contacts, and reduced primary porosity. Unstained, uncrossed nicols, 0.5-mm bar, sample from the Livingston 1 location.

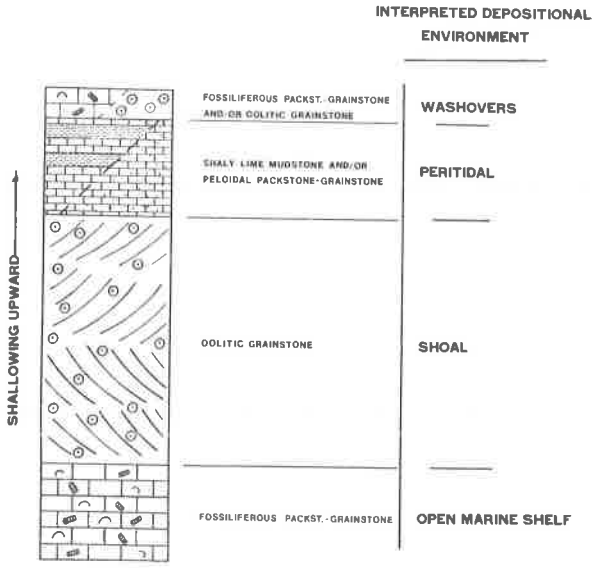

Figure 11. The idealized shallowing upward cycle of Monteagle lithologies.

decreasing water depth (Handford, 1979).

Tidal flat and supratidal environments developed in shallow-water low-energy areas adjacent to the oolite dune crests. The micrite producing/depositing environments presumably migrated over dune crests as a consequence of minor sea level changes due to storm, local tectonic, or eustatic changes in relative water depth. Intertidal deposits are represented by thin-bedded wackestones and peloidal packstone-grainstones, whereas supratidal deposits are represented by mudstones containing a wide range of fenestral fabrics and high percentage of dolomite. This textural variety is consistent with the great lateral complexity observed in many modern intertidal and supratidal areas.

Wackestone/micrite lithologies are overlain by fossiliferous packstone/grainstones suggesting a return to subtidal interior platform deposition.

Lateral variations between the individual cycles at the Cookeville and Livingston outcrops suggests that the epeiric sea deepened slightly from Livingstone 1 to Cookeville, resulting in a realm of dominantly shallow subtidal and extensive peritidal deposition to the south, and a realm of less extensive peritidal deposition to the north. The principal basis for this hypothesis is the relatively greater abundance of dolomite in samples at Cookeville.

A 5- to 10-foot shale unit (the La Follet Shale?) is commonly present near the top of the Monteagle throughout the Cumberland Plateau area (Fig. 8; and Peterson, 1962). This unit is interpreted to be a consequence of a clastic pulse into the area; a precursor of the Big Clifty (Hartselle) clastics that follow the Monteagle. The appearance of detrital quartz nuclei in oolite units above the La Follet shale marks the initial input of sand-sized clastics into the area. Deposition of the Monteagle was halted by progradation of the Big Clifty-Hartselle delta (Roberts and Lumsden, 1982).

Porosity

The compacted appearance of most fossiliferous packstone-grainstones as observed here and in the Ste. Genevieve Limestone (Choquette and Steinen, 1980) contrasts with the open uncompacted appearance of the associated oolitic grainstones. We believe that the turbulent, mud free, $CaCO_3$ super-saturated environment in which the Monteagle oolites formed was favorable to early, perhaps syndepositional cementation. On the other hand the deeper, quieter, muddier, less carbonate saturated environment of fossiliferous packstone-grainstone deposition did not favor early cement. Interpenetration and dissolution of adjacent grains is hindered after the

precipitation of cement because cement effectively prevents relative movement between grains. As a consequence the oolite grainstones were propped open and at least part of their original porosity, that part not destroyed by deposition of void filling spar, was preserved. In contrast the fossiliferous packstone-grainstones compacted markedly and the reduced remaining void was easily filled by pressolved carbonate.

CONCLUSIONS

The Monteagle Limestone of the study area is dominated by an oolitic grainstone lithology with an open uncompacted, petrographic texture. These oolites form the major unit in a lithologic sequence that repeats 8 to 10 times. This repetition may be a consequence of cyclic shallowing of marine waters from open shelf through shoal to tidal flat water depths. Features 105 km (65 mi) to the east, at the Jellico outcrop, suggest quieter, probably deeper water conditions on a marine shelf.

The oolite shoals trend NNE, roughly perpendicular to the trend of the controlling paleoshoal area.

The thick trends in net porosity overlie and are parallel to the NNE-SSW orientated *thin* trends in total thickness. This suggests that the best reservoir potential may be found where the oolite dunes have stacked up on pre-Monteagle highs (Monteagle thins). The ease of correlation of the lithologic cycles in the Monteagle, the abundance of oolite grainstone lithologies and the occurrence of NNE-SSW trends in net porosity suggests that the Monteagle has petroleum reservoir potential over the entire study area and that exploration both north and south of the currently delineated productive fairway may prove economic. The coincidence of Monteagle gas fields over Ft. Payne oil fields suggests that Monteagle production is an accidental by-product of Ft. Payne exploration. The Monteagle merits separate investigation.

ACKNOWLEDGMENTS

A grant from Amoco Production Co. supported costs incurred in this study. Robert Lindau of the Tennessee Division of Geology gave generously of his time and knowledge. Robert Milici of the Virginia Division of Mineral Resources reviewed the manuscript and made helpful suggestions.

REFERENCES CITED

Ball, M. M., 1967, Carbonate sand bodies of Florida and the Bahamas: Jour. Sed. Petrology, v. 37, p. 556-591.

Bathurst, R. G. C., 1976, Carbonate Sediments and Their Diagenesis (2nd ed.): New York, Elsevier, 658 p.

Carr, D. D., 1973, Geometry and origin of oolite bodies in the Ste. Genevieve Limestone (Mississippian) in the Illinois Basin: Indiana Dept. Natural Res. Geol. Surv. Bull. 48, 81 p.

Choquette, P. W., and Steinen, R. P., 1980, Mississippian nonsupratidal dolomite, Ste. Genevieve Limestone, Illinois Basin: evidence for mixed water dolomitization, *in* Zenger, D. H., Dunham, J. B., and Ethington, R. L., eds., Concepts and Models of Dolomitization: Soc. Econ. Paleontologists Mineralogists Spec. Pub. 28, p. 163-196.

Dunham, R. J., 1962, Classification of carbonate rocks according to depositional texture, *in* Ham, W. H., ed., Classification of Carbonate Rocks, A Symposium: Am. Assoc. Petroleum Geologists Mem. I, p. 108-121.

Gregory, P. G., 1981, Petrology and paleoenvironments of the Mississippian system exposed at Jellico, Tennessee [unpub. Masters thesis]: Memphis State Univ., 82 p.

Handford, C. R., 1978, Monteagle Limestone (Upper Mississippian)--oolitic tidal bar sedimentation in the Southern Cumberland Plateau: Am. Assoc. Petroleum Geologists Bull., v. 62, p. 644-656.

Keplinger and Associates, 1980, Natural gas reserve study, Fentress, Morgan, and Scott Counties, Tennessee: Open File Report, Tenn. Div. Geology.

Lindholm, R. C., and Finkleman, R. B., 1972, Calcite staining: semiquantitative determination of ferrous iron: Jour. Sed. Petrology, v. 42, p. 239-242.
Lumsden, D. N., and Chimahusky, J. S., 1979, Relationship between dolomite non-stoichiometry and carbonate facies parameters, *in* Zenger, D. H., Dunham, J. B., and Ethington, R. L., eds., Concepts and Models of Dolomitization: Soc. Econ. Paleontologists Mineralogists Spec. Publ. 28, p. 123-137.
Milici, R. C., Briggs, G., Knox, L. M., Sitterly, P. O., and Statler, A. T., 1979, The Mississippian and Pennsylvanian (Carboniferous) Systems in the United States-Tennessee, *in* Skehan, J.W., ed., The Mississippian and Pennsylvanian Systems in the United States: U. S. Geological Survey Prof. Paper 1110-A, p. 11-37.
Newell, N. D., Purdy, E. G., and Imbrie, J., 1960, Bahamian oolitic sand: Jour. Geology, v. 68, p. 481-497.
Norman, C.D., 1981, Petrology and paleoenvironments in the Monteagle Limestone (Mississippian), Northcentral Tennessee [unpub. Masters thesis]: Memphis State Univ., 97 p.
Peterson, M. N. A., 1962, The mineralogy and petrology of Upper Mississippian carbonate rocks of the Cumberland Plateau in Tennessee: Jour. Geology, v. 70, p. 1-31.
Reid, B. J., 1981, A subsurface study of the Monteagle Limestone: Northeast Tennessee [unpub. Masters thesis]: Memphis State Univ., 80 p.
Roberts, J. B., and Lumsden, D. N., 1982, The Big Clifty (Hartselle) Formation (Mississippian) in southeast Tennessee, petrology lithofacies and origin: Southeastern Geology, v. 23, p. 71-81.
Shinn, E. A., 1964, Recent dolomite, Sugarloaf Key, Florida, *in* Ginsburg, R. N., ed., South Florida Sediments: Geol. Soc. America Guidebook, Field Trip I, Ann. Mtg., Florida, p. 26-33.
Shinn, E. A., 1968, Practical significance of birdseye structures in carbonate rocks: Jour. Sed. Petrology, v. 38, p. 215-223.
Shinn, E. A., Lloyd, R. M., and Ginsburg, R. N., 1969, Anatomy of a modern carbonate tidal flat, Andros Island, Bahamas: Jour. Sed. Petrology, v. 39, p. 1202-1228.
Stearns, R., 1963, Monteagle Limestone, Hartselle Formation, and Bangor Limestone--a new Mississippian nomenclature for use in Middle Tennessee, with a history of its development: Tenn. Div. Geol. Info. Circ. 11, 18 p.
Thomas, W. A., 1972, Mississippian stratigraphy of Alabama: Alabama Geol. Survey, Mon. 12, p. 121.
Vail, P. R., 1959, Stratigraphy and lithofacies of Upper Mississippian rocks in the Cumberland Plateau [Ph.D. dissertation]: Northwestern Univ., 148 p.
Webb, E. J., 1972, Stratigraphic relationships of certain Mississippian age pools in southeastern Kentucky and northeastern Tennessee: Kentucky Geol. Surv. Spec. Pub. 21, Ser. X, p. 50-58.